


RESEARCH ARTICLE

A β plaques do not protect against HSV-1 infection in a mouse model of familial Alzheimer's disease, and HSV-1 does not induce A β pathology in a model of late onset Alzheimer's disease

Olga V. Bocharova^{1,2} | Aidan Fisher^{1,2} | Narayan P. Pandit^{1,2} | Kara Molesworth^{1,2} |
Olga Mychko^{1,2} | Alison J. Scott³ | Natallia Makarava^{1,2} | Rodney Ritzel⁴ |
Iliia V. Baskakov^{1,2} 

¹Center for Biomedical Engineering and Technology, University of Maryland School of Medicine, Baltimore, Maryland, USA

²Department of Anatomy and Neurobiology, University of Maryland School of Medicine, Baltimore, Maryland, USA

³Department of Microbial Pathogenesis, University of Maryland School of Dentistry, Baltimore, Maryland, USA

⁴Department of Anesthesiology and Center for Shock, Trauma and Anesthesiology Research (STAR), University of Maryland School of Medicine, Baltimore, Maryland, USA

Correspondence

Iliia V. Baskakov, Department of Anatomy and Neurobiology, University of Maryland School of Medicine, Baltimore, Maryland, 21201, USA.

Email: baskakov@som.umaryland.edu

Funding information

Infectious Diseases Society of America; IDSA Foundation

Abstract

The possibility that the etiology of late onset Alzheimer's disease is linked to viral infections of the CNS has been actively debated in recent years. According to the antiviral protection hypothesis, viral pathogens trigger aggregation of A β peptides that are produced as a defense mechanism in response to infection to entrap and neutralize pathogens. To test the causative relationship between viral infection and A β aggregation, the current study examined whether A β plaques protect the mouse brain against Herpes Simplex Virus 1 (HSV-1) infection introduced via a physiological route and whether HSV-1 infection triggers formation of A β plaques in a mouse model of late-onset AD that does not develop A β pathology spontaneously. In aged 5XFAD mice infected via eye scarification, high density of A β aggregates did not improve survival time or rate when compared with wild type controls. In 5XFADs, viral replication sites were found in brain areas with a high density of extracellular A β deposits, however, no association between HSV-1 and A β aggregates could be found. To test whether HSV-1 triggers A β aggregation in a mouse model that lacks spontaneous A β pathology, 13-month-old hA β /APOE4/Trem2*R47H mice were infected with HSV-1 via eye scarification with the McKrae HSV-1 strain, intracranial inoculation with McKrae, intracranial inoculation after priming with LPS for 6 weeks, or intracranial inoculation with high doses of McKrae or 17syn + strains that represent different degrees of neurovirulence. No signs of A β aggregation were found in any of the experimental groups. Instead, extensive infiltration of peripheral leukocytes was observed during the acute stage of HSV-1 infection, and phagocytic activity of myeloid cells was identified as the primary defense mechanism against HSV-1. The current results argue against a direct causative relationship between HSV-1 infection and A β pathology.

KEYWORDS

5XFAD mice, Alzheimer's disease, amyloid precursor protein, A β aggregates, hA β /APOE4/Trem2*R47H mice, herpes simplex virus 1, infiltrating myeloid cells, microglia

1 | INTRODUCTION

Alzheimer's disease (AD) is the most common fatal neurodegenerative disease, with more than 90% of all AD cases being late-onset and believed to be sporadic in origin. According to the amyloid cascade hypothesis, aggregation of A β peptides, the proteolytic fragments of Amyloid Precursor Protein (APP), triggers a pathological cascade of events leading to AD [1–3]. An alternative to the amyloid cascade hypothesis is the hypothesis that viral and microbial pathogens of the CNS are involved in the etiology of late-onset AD [4–6]. The antiviral protection hypothesis proposes that CNS pathogens trigger aggregation of A β peptides that are produced as a defensive mechanism in response to infection [7–10].

Among the broad range of pathogens, herpesviruses emerged as one of the leading pathogens linked to late onset AD [7, 11–23]. With increased scrutiny, the topic of the association of herpesviruses to late onset AD has become increasingly controversial. Transcriptomic analysis of several brain banks revealed a link between herpesviruses HHV-6A and HHV7 and AD [24]. However, reanalysis of the same datasets using different statistical methods [25], as well as analysis of additional cohorts did not support an association between herpesviruses and AD [26]. Considering that viral infections and AD progression often coincide because both are common in aged brains, and that infections might be secondary to AD due to a disrupted blood brain barrier, establishing a causative relationship between pathogens and A β pathology is challenging. A β pathology is considered as one of the earliest preclinical hallmarks of AD that precedes the clinical onset by up to 15 years [27, 28], so elucidating molecular mechanisms that trigger A β pathology is very important for understanding AD etiology.

To test a causative relationship between HSV-1 infection and A β plaques, the current study examined (i) whether A β plaques protect mouse brains from HSV-1 infection introduced via a physiological route, and (ii) whether HSV-1 infection triggers A β plaques in brains of a mouse model of late-onset AD that does not develop A β pathology spontaneously. In aged 5XFAD mice infected via eye scarification, high density of A β aggregates did not improve survival time or rate when compared with the age-matched wild type controls. Moreover, while viral replication sites were seen in brain areas with a high density of extracellular A β deposits, no association between HSV-1 and A β aggregates could be found. For testing whether HSV-1 infection triggers A β plaques, a mouse model referred to as hA β that expresses humanized A β sequence (hA β) within the mouse *APP* gene under endogenous promoter along with humanized *APOE4* knock-in substitution and the R47H point mutation knocked into mouse *Trem2* gene was used. This model was chosen because APOE4 and Trem2 R47H variants significantly increase the risk, yet are not sufficient to cause late-onset AD at a 100% rate. Moreover,

considering previous studies illustrating that APOE4 exacerbates A β pathology via enhancing amyloid deposition during the early, seeding stages of A β aggregation [29, 30], we anticipated that mice expressing APOE4 would be susceptible to develop A β pathology upon viral infection. A systematic search of conditions for triggering A β aggregation was conducted, where 13-month-old hA β mice were infected with HSV-1 via (i) eye scarification with McKrae strain, (ii) IC inoculation with McKrae, (iii) IC inoculation with McKrae after priming with LPS for 6 weeks, or (iv) IC inoculation with high doses of McKrae or 17syn+ strains. No signs of A β aggregation were found in any of the experimental groups. Instead, extensive infiltration of peripheral leukocytes was observed during the acute stage of HSV-1 infection, and phagocytic activity of myeloid cells was identified as the primary defense mechanism against HSV-1.

2 | METHODS

2.1 | Experimental models

Male and female 5XFAD mice [B6SJL-Tg(APPswFl-Lon, PSEN1*M146L*L286V) 6799Vas/Mmjax, [Jax.org](https://jax.org) catalog # 34840] and WT littermates were group-housed together in random ratios, three to five mice per cage. The ratio of males and females for both 5XFAD and WT littermates was random in each experiment. hA β mice (hAPP/APOE4/Trem2*R47H, [Jax.org](https://jax.org) catalog #030670) carry a humanized *APOE4* knock-in substitution, humanized *APP* (hAPP) gene and R47H point mutation of the *Trem2* gene. The ratio of males and females for hA β mice was random in each experiment. All mice were kept on a 12 h light/dark cycle. The study was carried out in accordance with the recommendations in the Guide for the Care and Use of Laboratory Animals of the National Institutes of Health. The animal protocol was approved by the Institutional Animal Care and Use Committee of the University of Maryland, Baltimore (Assurance Number: A32000-01; Permit Number: 0419007).

2.2 | Production and titration of HSV-1 stocks

HSV-1 17Syn+ and McKrae strains were propagated in Vero cell culture with an initial multiplicity of infection (MOI) of 0.01 PFU/cell in serum-free medium. After 2 h of incubation at 37°C, the viral inoculum was aspirated, and the cell culture was supplemented with fresh DMEM medium with 5% newborn calf serum. Cells were incubated for 2 to 3 days until 100% of the cells displayed cytopathic effects. After one freezing and thawing cycle, cells were sonicated five times for 30 sec using a Misonix S-4000 sonicator at 600 W output, letting the cell

suspension cool on ice for 1 min between sonications. After centrifugation of the Vero cell lysate at 12000 \times g for 10 min at 4°C, virus-containing supernatant was mixed with 10% sterile BSA solution to a final concentration of 2% BSA, and supplemented with 10x PBS to a final concentration of 1x PBS (with 137 mM of NaCl and 3 mM KCl). Viral stock was split into smaller aliquots in screw-capped cryovials and stored at -80°C. In parallel, mock control stock solution was made from noninfected Vero cells lysate. The HSV-1 17 Syn+ strain was a generous gift from Dr. Krause (FDA) and the HSV-1 McKrae strain was a generous gift from Dr. Cohen (NIH).

Viral titer was measured by a standard plaque assay on Vero cell culture under 0.9% agar layer. 10-fold serial dilutions in 1 ml serum-free medium were added to the corresponding well of a 6-well plate in duplicates and incubated for 2 h with swirling every 30 min. Plates underwent plaque count after 2–3 days of incubation. Cells were fixed with methanol and stained with 0.5% Crystal Violet in 25% methanol for plaque visualization. To determine the titer of the stock, the number of plaques in duplicate was averaged for a given dilution.

2.3 | Inoculation of HSV-1

5XFAD APP/PS1 transgenic mice (Oakley et al. [35]) overexpress FAD mutant forms of human APP (the Swedish mutation: K670N, M671L; the Florida mutation: I716V; the London mutation: V717I) along with PS1 (M146L; L286V) transgenes under the transcriptional control of the neuron-specific mouse Thy1 promoter (Tg6799 line), and produce elevated levels of A β 42 peptide. 5XFAD lines (with B6SJLF1/J genetic background) were purchased from Jackson Laboratory and maintained by crossing hemizygous 5XFAD transgenic males with B6SJLF1/J female breeders. All pups were genotyped using Transnetyx genotypic services (Cordova, TN, USA). All 5XFAD transgenic mice were hemizygous with respect to the transgene. Control animals were caged separately from the animals inoculated with HSV-1.

McKrae and 17Syn+ inoculation stocks were prepared in PBS containing 137 mM of NaCl, 3 mM KCl and 2% sterile BSA and supplemented with antibiotics-antimycotics concentrate (Invitrogen). Immediately before inoculation, stocks were diluted with PBS-BSA sterile solution to the required titer. For intracerebral inoculation (IC), each animal received a single 20 μ l of inoculum under 2.5% isoflurane anesthesia, in the center of the left hemisphere, 2 mm away from the sagittal suture. The injection depth of 2 mm was achieved using a needle length stopper made from a needle cap. All animals handled IC injections well and fully recovered within 1 h.

For a challenge via eye scarification, HSV-1 was administered via a cornea scarification procedure. Before cornea scarification, each animal was anesthetized under

2.5% isoflurane. The cornea surface was gently scarified using a 22-gauge needle by drawing a hashtag sign. The viral inoculum was applied in a volume of 5 μ l to a surface of an eye by a pipette and allowed to absorb for approximately 5 min.

After inoculation via IC or eye scarification, animals were weighed and observed daily for the following signs of acute Herpes Simplex virus encephalitis: eye and face inflammation, walking difficulty, tremor, hunched posture, and weight loss. The animals were euthanized when they demonstrated the severe aforementioned clinical signs along with 20% loss of their body weight, as determined relative to weights measured before virus inoculation.

2.4 | Inoculation of prions

For infecting hA β mice with prions, mouse-adapted prion strain SSLOW that causes widespread neuroinflammation and is characterized by short incubation time to disease was used [31, 32]. Using isoflurane anesthesia, 13-month old hA β female and male mice were subjected to intraperitoneal inoculation of 1% brain homogenate, prepared in PBS (pH 7.4) using terminally ill SSLOW-infected mice. Brain material from the 5th passage of SSLOW in mice was used for inoculations [31]. Inoculation volume was 200 μ l. Animals were regularly observed for signs of neurological impairment: abnormal gate, hind limb clasp, lethargy, and weight loss. Mice were considered terminally ill when they were unable to rear and/or lost 20% of their weight.

2.5 | LPS purification and inoculation

Ultrapurified LPS was extracted from *E. coli* strain C5 [BORT] (ATCC 700973), a strain producing smooth LPS with a hexaacylated, bis-phosphorylated lipid A base. Briefly, pellets for LPS extraction were harvested from large cultures grown in 1 L volumes of lysogeny broth with 1 mM MgCl₂, shaking at 180 RPM, for 16–18 h. The large batch hot phenol/water extraction method was used to extract LPS followed by a lipid cleanup (Folch method) and lipoprotein cleanup (Hirshfield method) [33]. Lyophilized product was characterized as a Toll-like Receptor 4 (TLR4) agonist in HEK-Blue mTLR4 reporter cell lines (Invivogen). Product was quantified by dry weight. Lipid A structure was confirmed using the Fast Lipid A Analysis Technique. Single-use dose aliquots were made to deliver 1 mg/kg in 100 μ l PBS. All related chemicals were sourced from Sigma-Aldrich (St. Louis, MO). Cell culture reagents were sourced from Invivogen (HEK-Blue mTLR4, SEAP reporter kit) or Gibco (DMEM, FBS, PBS) and cultured according to the Invivogen protocols.

LPS was administered intraperitoneally (IP) to 13-month old mice once per week for 6 consecutive weeks.

Each week, the same dose of LPS (1 mg/kg of weight) was inoculated using stock solution 0.3 mg/ml in PBS with 0.9% saline. PBS with 0.9% saline was administered IP to age-matched controls.

2.6 | Histopathology and immunofluorescence

After euthanasia by CO₂ asphyxiation, brains were immediately extracted and kept ice-cold during dissection. Brains were sliced using a rodent brain slicer matrix (Zivic Instruments, Pittsburg, PA), formalin-fixed and embedded in paraffin. Formalin-fixed brains from SSLOW-infected mice were treated for 1 h in 96% formic acid before being embedded in paraffin, to deactivate prion infectivity. 4 μm sections were produced using a Leica RM2235 microtome (Leica Biosystems, Buffalo Grove, IL), mounted on slides and processed for immunohistochemistry.

Rehydrated slides were subjected to the procedure of epitope exposure that involved hydrated autoclaving at 121°C for 20 min in trisodium citrate buffer, pH 6.0, with 0.05% Tween 20. To aid PrP^{Sc} epitope exposure, in addition to hydrated autoclaving, slides of SSLOW-infected mice were treated with concentrated formic acid for 5 min. All antibodies used in this study are listed in the Key Resources Table 1. Immunofluorescence detection was performed with AlexaFluor-488 or AlexaFluor-546 labeled secondary antibodies. An autofluorescence eliminator (Sigma-Aldrich, St. Louis, MO) was used according to the original protocol to reduce background fluorescence. Fluorescent images were collected using an inverted Nikon Eclipse TE2000-U microscope (Nikon Instruments Inc., Melville, NY) equipped with an illumination system X-cite 120 (EXFO Photonics Solutions Inc., Exton, PA) and a cooled 12-bit CoolSnap HQ CCD camera (Photometrics, Tucson, AZ).

2.7 | Western blot

Membrane-soluble APP from 30 mg of temporal lobe cortex was extracted using Mem-PER™ Plus Membrane Protein Extraction Kit (Thermo Scientific, # 89842). Briefly, brain tissue was homogenized in 0.5 ml of Permeabilization buffer supplemented with Protease Inhibitor Cocktail (Sigma, #P1860). After 10 min incubation on ice, samples were centrifuged at 15,000×g for 15 min at 4°C and pellet was resuspended in 0.5 ml of Solubilization Buffer, supplemented with Protease Inhibitor Cocktail. After 30 min incubation at 4°C and centrifugation the supernatant containing solubilized membrane and membrane-associated proteins was transferred to a new tube. All samples were subjected to protein concentration determination using Pierce BCA Protein Assay Kit (Thermo Scientific, #23225) and diluted to a final concentration 50 μg per SDS PAGE probe. Proteins from gel were transferred on PVDF membrane (Bio Rad, #10026933) using Trans-Blot Turbo transfer system, with 1.3A, 25 V, 7 min transfer setting. After transfer membrane was boiled for 5 min in PBS and stained with 6E10 (1/1000) and goat-a-mouse HRP-labelled (1/5000) antibodies. Reaction was visualized with Immobilon Forte Western HRP Substrate (Millipore, #WBLUF0500) and image was taken in digital darkroom FluorChem M (Protein Simple, Santa Clara, CA).

2.8 | Flow cytometry

After transcardial perfusion with 40 ml of ice-cold sterile phosphate buffered saline (PBS), the brain hemisphere (left) of each mouse was passed through a 70 μm nylon Cell Strainer (Corning #431751) using FACS medium DMEM (Invitrogen, #11885084), supplemented with 2% FBS (Invitrogen, #16140071). CNS tissue was then

TABLE 1 Key resources immunofluorescence antibody

| Antigen | Label/species | Source | Catalog # |
|--|-----------------|---------------------------|--------------|
| gD | Mouse | Abcam | Ab6507 |
| HSV-1,2 | Rabbit | Abcam | Ab9533 |
| Iba1 | Goat | Novus | NB100-1028SS |
| Iba1 | Rabbit | FUGIFILM Wako Chemicals | 013-27691 |
| GFAP | Rabbit | Cell Signaling Technology | 07/2019 |
| 6E10 | Mouse | Bio Legend | 803,001 |
| Gal3 | Rat | Santa Cruz Biotechnology | Sc-23,938 |
| SAF-84 | Mouse | Cayman Chemical | #189775 |
| Donkey-anti-mouse | Alexa Fluor 488 | Invitrogen | A21202 |
| Donkey-anti-rabbit | Alexa Fluor 488 | Invitrogen | A21206 |
| Goat-anti-rabbit | Alexa Fluor 546 | Invitrogen | A11010 |
| Goat-anti-mouse | Alexa Fluor 546 | Invitrogen | A11003 |
| VECTASHIELD Antifade Mounting medium with DAPI | DAPI | VECTOR Laboratories, Inc. | H-1200 |

enzymatically digested in 5 ml using DNase (0.6 mg/ml; Thermo Scientific #J62229MB), Collagenase/Dispase (30 μ g/ml; Sigma 10269638001), and Papain (6 U, Sigma #P3375) for 1 h at 37°C in a water bath, with intermediate shaking every 15 min. Tissue homogenates were centrifuged at 1500 rpm for 5 min at 4°C. After washing with cold DPBS, buffer cells were split for staining into FACS tubes. Cells were blocked with mouse Fc Block (BD Biosciences) before staining with primary antibody-conjugated fluorophores and viability dye (CD45, CD11b, Ly6C, Zombie Aqua—see Flow Cytometry Key Resources Table 2) purchased from BioLegend (San Diego, CA). Later cells were washed and fixed/permeabilized with Cytotfix/cytoperm Kit (BD Biosciences) according to the manufacturer's instructions. For intracellular staining, cells were incubated with CD68 and NeuN in Permeabilization/Wash buffer (BD Biosciences) for 30 min. Cells were then washed twice with FACS buffer (DPBS supplemented with 2% FBS) and fixed with 2% paraformaldehyde (PFA).

For live/dead cell discrimination, a fixable viability dye, Zombie Aqua (BioLegend), was dissolved in DMSO according to the manufacturer's instructions and added to cells in a final concentration of 1:200. Data were acquired on an LSRII using FACSDiva 6.0 (BD Biosciences, San Jose, CA) and analyzed using FlowJo (Tree Star, San Carlos, CA). A standardized gating strategy was used to identify brain-resident microglia (MG, CD45^{int}CD11b⁺Ly6C⁻), peripheral infiltrating myeloid cells (iMy, CD45^{hi}CD11b⁺Ly6C⁺) and lymphocytes (iLym, CD45^{hi}CD11b⁻). Fluorescence minus one (FMO) control samples were used to determine the positivity of each antibody. Cell count estimations were performed using Precision Count Beads (50 μ l/test; BioLegend) according to the manufacturer's instructions.

Data were combined from two independent experiments. For all experiments, $n = 3-5$ /group. Data were analyzed using two-way ANOVA with Sidak's multiple comparisons test, with individual variances computed for each comparison (Graph Pad Prism 9.1) and expressed as mean \pm SD.

2.9 | Phagocytosis bead assay

Phagocytic activity of myeloid cells was performed as described [34] with minor modification. Briefly, yellow-green and red fluorescent carboxylate-modified polystyrene latex beads (1 and 0.5 μ m mean diameter, Sigma) were added to freshly isolated cells in a final dilution of 1:100 (in RPMI). After 1 h incubation at 37°C, the cells were washed three times, resuspended in FACS buffer, treated with Fc Block, stained with surface markers, and fixed in PFA.

2.10 | Quantification and statistical analysis

To quantify 6E10 signal coverage, image pixels from cortex area taken under $\times 20$ magnification were thresholded after automatic subtraction of background, using ImageJ (Fiji) software. Nonspecific to 6E10 signals from blood vessels were manually deleted before thresholding. The signal coverage was measured as % of area for images. The data was first tested for normality using D'agostino-Pearson test. Statistical analysis was performed with two-tailed t -test using Prism 9.1 software (GraphPad Software, Inc., San Diego, CA) and expressed as mean \pm SD; the level of significance was set at $p < 0.05$.

For quantification of APP expression in individual cells images were taken using Leica SP8 Multiphoton Confocal Microscope under $\times 60$ magnification as a group of tiles with the same exposure time and laser power settings. The motor cortex area was chosen for quantification for all groups. After subtraction of background, Region Of Interest (ROI) 80 px in diameter was drawn around neurons and raw pixel intensity was calculated. Confocal images were processed using WCIF ImageJ software (National Institute of Health, Bethesda, MD, United States). The differences in 6E10 signal intensity in hA β and 5XFAD brains were compared using Mann-Whitney nonparametric test using GraphPad Prism software.

TABLE 2 Flow cytometry key resources

| Marker | Label | Ab clone | Source | Notes |
|----------------------------|--------------|----------|------------------------|---|
| CD45 | BV421 | 30-F11 | Bio Legend #103133 | |
| CD11b | APC/Fire 750 | M1/70 | Bio Legend #101261 | |
| Ly6c | Alexa 488 | HK1.4 | Bio Legend #128021 | |
| Ly6c | Alexa 700 | HK1.4 | Bio Legend #128023 | |
| CD68 | PE | FA-11 | Bio Legend #137013 | |
| NeuN | Alexa 647 | 1b7 | Bio Legend #834502 | Home labeled with A647 kit (Invitrogen #A20186) |
| Zombie dye | Aqua | | Bio Legend #423101 | |
| Precision Count Beads | | | Bio Legend #424902 | |
| 1 μ m beads | FITC | | Sigma #L3280 | |
| 0.5 μ m beads | PE-Texas Red | | Sigma #L4655 | |
| Mouse BD Fc Block™ | | | BD Biosciences #553142 | |
| Cytotfix/cytoperm Soln Kit | | | BD Biosciences #554714 | |

Statistical analysis of survival curves was performed using GraphPad Prism software. Survival curves were compared using a Log-rank (Mantel-Cox) test. Differences with the p values >0.05 were considered lacking statistical significance. Group statistics for flow cytometry data were analyzed by an ordinary 2-way ANOVA with Šidák's multiple comparisons test, with individual variances computed for each comparison and expressed as mean \pm SD ($*p < 0.05$). Quantification of intracellular APP/A β levels was calculated using unpaired nonparametric two-tailed Mann-Whitney U test ($*p < 0.05$).

3 | RESULTS

3.1 | 5XFAD genotype and A β plaques do not protect against HSV-1 infection via a physiological route

To test whether A β peptides and A β plaques protect against HSV-1 infection upon challenges via physiological route, 14-month-old male and female 5XFAD mice along with littermate B6SJL (WT) control mice were infected with McKrae strain of HSV-1 via eye scarification. By 14-months of age, 5XFADs accumulate high amounts of A β 40 and A β 42 peptides and show a high density of A β plaques across multiple brain regions [35]. At the dose of 6.8×10^4 PFUs per animal, the survival curves were the same for 5XFAD and WT groups (Figure 1A). At 3.4×10^5 PFUs, the WT group showed slightly longer survival time relative to 5XFADs, yet the difference between the two cohorts was at the borderline of statistical significance (Figure 1B).

Upon exposure via eye scarification, HSV-1 is transported to trigeminal ganglion before reaching the brain [36]. For testing whether brains were infected upon eye scarification, a series of coronal and sagittal slices were prepared and co-immunostained using anti-HSV1 antibodies (referred to as a-HSV1) that recognize viral replication centers [37, 38] and anti-gD antibodies that detect glycoproteins D of the HSV-1 envelope. Several areas including the piriform cortex, amygdala cortex and olfactory tubercle were consistently found to be infected in both, 5XFAD and WT control animals (Figure 2A). As expected, a-HSV1 detected replication centers and colocalized with nuclei of infected cells, whereas anti-gD labeled the cytoplasm of a-HSV1-positive cells and pericellular spaces in the vicinity of the a-HSV1-positive cells (Figure 2A). Noninfected age-matched 5XFAD lacked staining with a-HSV1 and anti-gD (Figure 2B). The fact that the same brain areas were affected in both 5XFAD and WT groups, along with the result that the 5XFAD genotype did not improve survival rate or time when compared with the WT cohort, suggests that A β peptides and A β aggregates do not interfere with viral spread.

To test whether HSV-1 co-localizes with A β aggregates, infected 14-month-old 5XFADs were co-immunostained

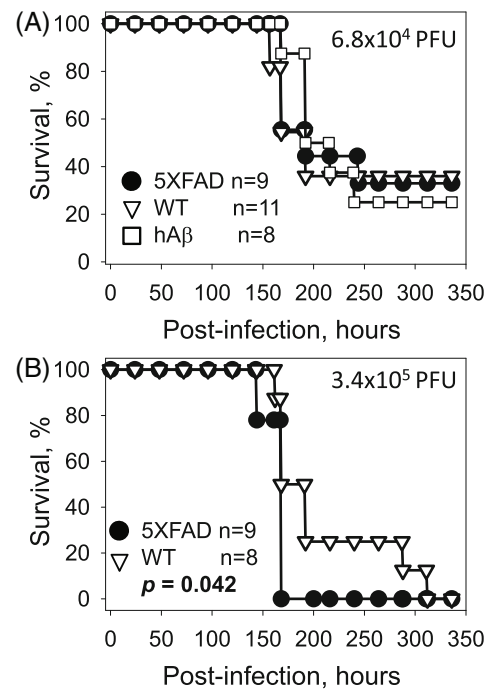
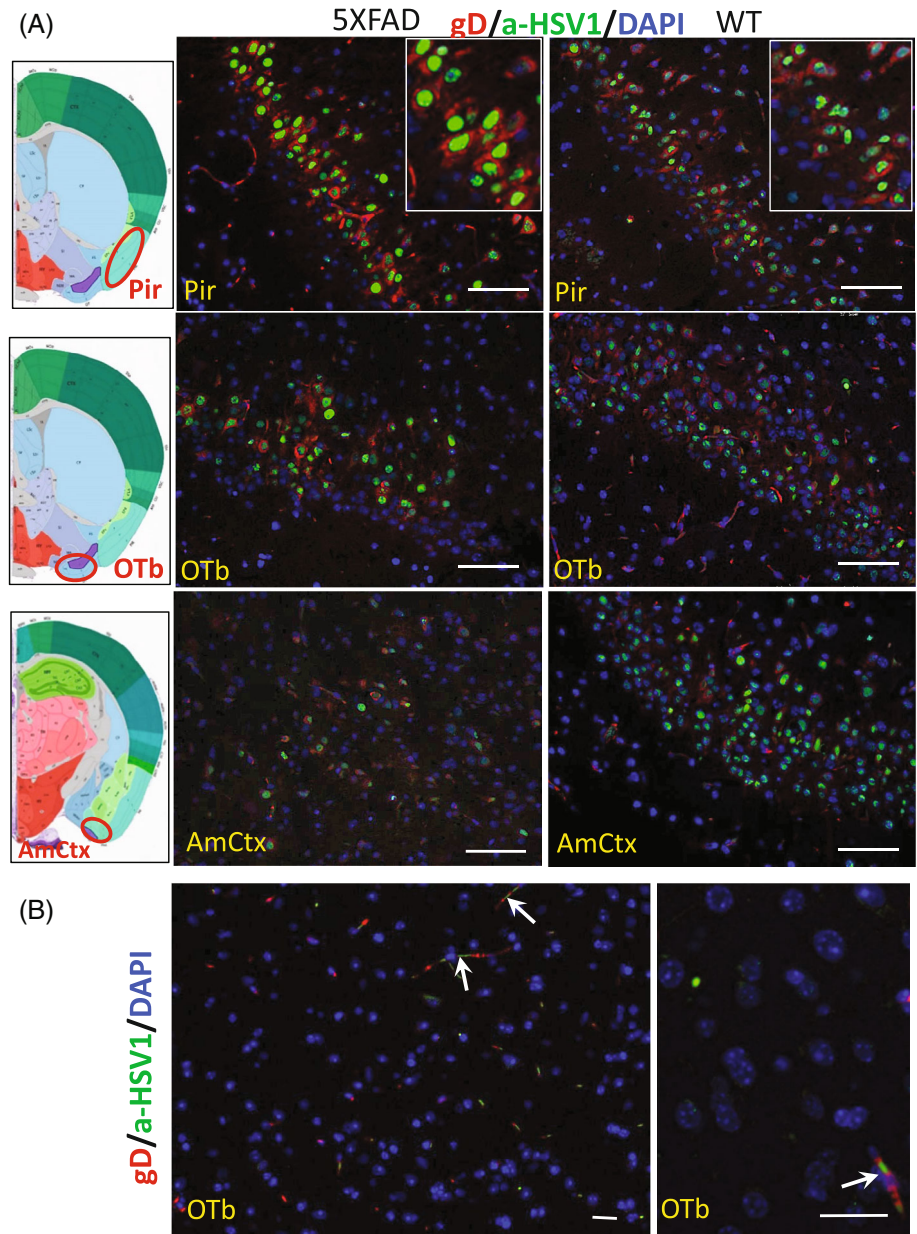


FIGURE 1 Dose–response of 5XFAD and hA β mouse models to HSV-1 infection via eye scarification. Survival curves for 14-month-old 5XFAD (black circles) and wild-type B6SJL littermate (WT, white triangles) mice challenged via eye scarification with 6.8×10^4 PFUs (A) or 3.4×10^5 PFUs (B) of McKrae strain per mouse. Survival curve for 12-month-old hA β mice (white squares) challenged via eye scarification with 6.8×10^4 PFUs (A). In A, $n = 5$ males + 4 females for 5XFAD and $n = 10$ males + 1 female for WT. In B, $n = 3$ males + 6 females for 5XFAD and $n = 3$ males + 5 female for WT. 5XFAD and WT littermate mice were caged together in random ratios. Individual plots show independent experiments with the number (n) of animals of each genotype indicated. Statistical significance (p) was calculated using the log-rank (Mantel-Cox) test.

using a-HSV1 antibodies paired with anti-A β antibody 6E10 (epitope aa 4–9 of the A β peptides) or anti-gD antibodies paired with another anti-A β antibody H31L21 (specific to A β 1–42, but not A β 1–40). H31L21 stains only dense core of A β plaques containing A β 1–42 peptide [38], whereas 6E10 reacts with a broad range of A β aggregates including amorphous and diffuse aggregates along with A β plaques. Both A β plaques and diffuse extracellular aggregates were found in the olfactory tubercle along with numerous a-HSV1- and gD-positive cells (Figure 3A). While some a-HSV1- and gD-positive cells were in close proximity to extracellular A β aggregates and plaques, no association between HSV-1 and A β aggregates could be found (Figure 3A). Infected WT control showed a spread of HSV-1 in a manner similar to that of 5XFAD, but lack 6E10- or H31L21-positive aggregates, confirming the specificity of detection of A β in aggregated states (Figure 3B). Noninfected 5XFADs lacked a-HSV1 and gD immunoreactivity confirming the specificity of HSV-1 detection (Figure 2B). Lack of association between A β aggregates and HSV-1 supports the idea that A β does not entrap the

FIGURE 2 Upon challenge via eye scarification, HSV-1 infection spreads to several brain areas. Co-immunostaining for HSV-1 replication centers (a-HSV1 antibody, green) and gD (anti-gD antibody, red) along with nuclei (DAPI, blue) in 14-month-old 5XFAD ($n = 7$ mice) and WT mice ($n = 7$ mice) challenged via eye scarification with 6.8×10^4 PFUs of McKrae (A), or in noninfected 14-month-old 5XFAD ($n = 6$ mice) (B). Animals were examined at 160–250 h postinfection. AmCtx, amygdala cortex; OTb, olfactory tubercle; Pir, piriform cortex. Insets in A show high magnification images. Arrows point at staining of blood vessels. Scale bars = 50 μ m in A and 20 μ m in B.



virus and does not interfere with its spread to the CNS upon infection.

3.2 | New triple mutant mouse strain for testing a causal relationship between HSV-1 infection and A β pathology

The majority of mouse models of familial AD, including 5XFAD, develop AD-specific pathology such as A β plaques spontaneously and independently of viral infections of CNS. Spontaneous development of plaques early in life poses limitations for testing a causative relationship between viral infection and AD pathology. For probing this causative relationship, we

selected a triple mutant mouse strain that carries a humanized *APOE4* knock-in substitution, the R47H point mutation knocked into mouse *Trem2* gene and humanized A β sequence (hA β) within the mouse *APP* gene. The triple mutant strain hA β /APOE4/*Trem2**R47H will be referred to as hA β . This mouse model expresses the variants of *APOE* and *Trem2* genes that significantly increase the risk of late-onset AD, yet are not sufficient to cause AD at a 100% rate. The human A β generated by this model is expected to be more aggregation prone than mouse A β . Because the *APP* gene is expressed under the native promoter, the hA β model is also physiologically more relevant than the 5XFAD model with respect to the level and pattern of the expression of *APP*.

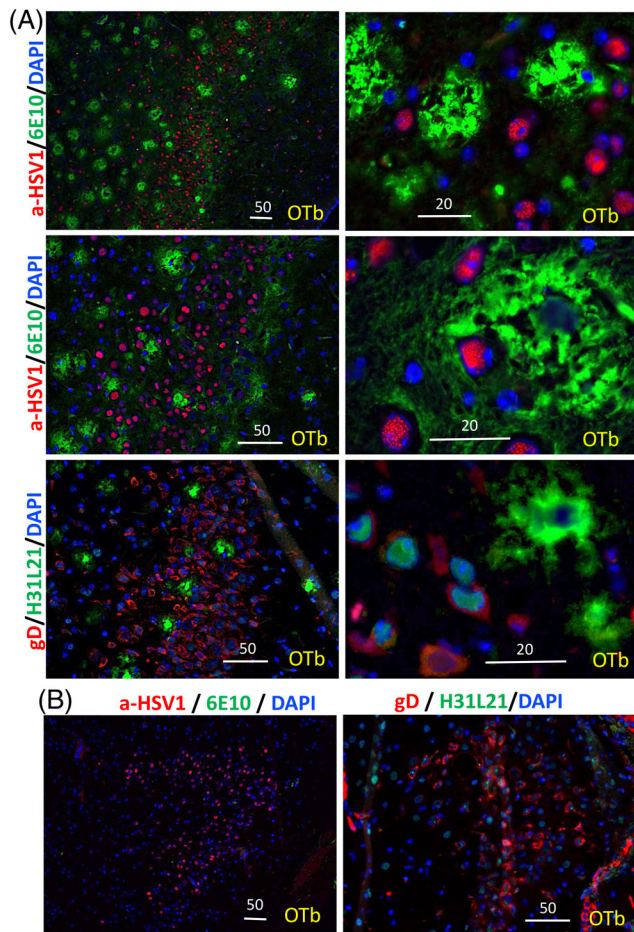


FIGURE 3 Lack of association between HSV-1 and A β aggregates in aged 5XFAD mice. Co-immunostaining for A β aggregates (6E10 antibody, green) and HSV-1 virus (a-HSV1 antibody, red), or A β plaques (H31L21 antibody, green) and HSV-1 virus (anti-gD antibody, red) along with nuclei (DAPI, blue) in 14-month-old 5XFAD mice ($n = 9$ mice) (A) or WT mice ($n = 6$ mice) (B) infected with 3.4×10^5 PFUs per mouse via eye scarification. OTb, olfactory tubercle. Scale bars = 50 or 20 μ m.

As expected, in hA β mice, the expression level of APP was considerably lower relative to expression in the 5XFAD model (Figure 4A). Nevertheless, cellular APP can be detected using staining with 6E10 throughout the brain in the hippocampus, cortex, thalamus, hypothalamus and stem (Figure 4B, C). In contrast to the 5XFAD model, in 1-year old hA β mice, A β peptides were not detectable by Western blot (Figure 4A). No signs of A β plaques or neuroinflammation could be observed by immunohistochemistry in 1-year old hA β mice (Figure 4B). The oldest, 22- to 24-month-old mice in the hA β cohort did not show any signs of A β aggregation or plaques (Figure 4C). Moreover, as judged by Iba1 staining, the majority of microglia/macrophages displayed ramified morphology, typical for their homeostatic state (Figure 4B, C). Lack of A β aggregates or overt neuroinflammation upon normal aging offers an opportunity for testing whether HSV-1 infection of CNS triggers A β pathology de novo.

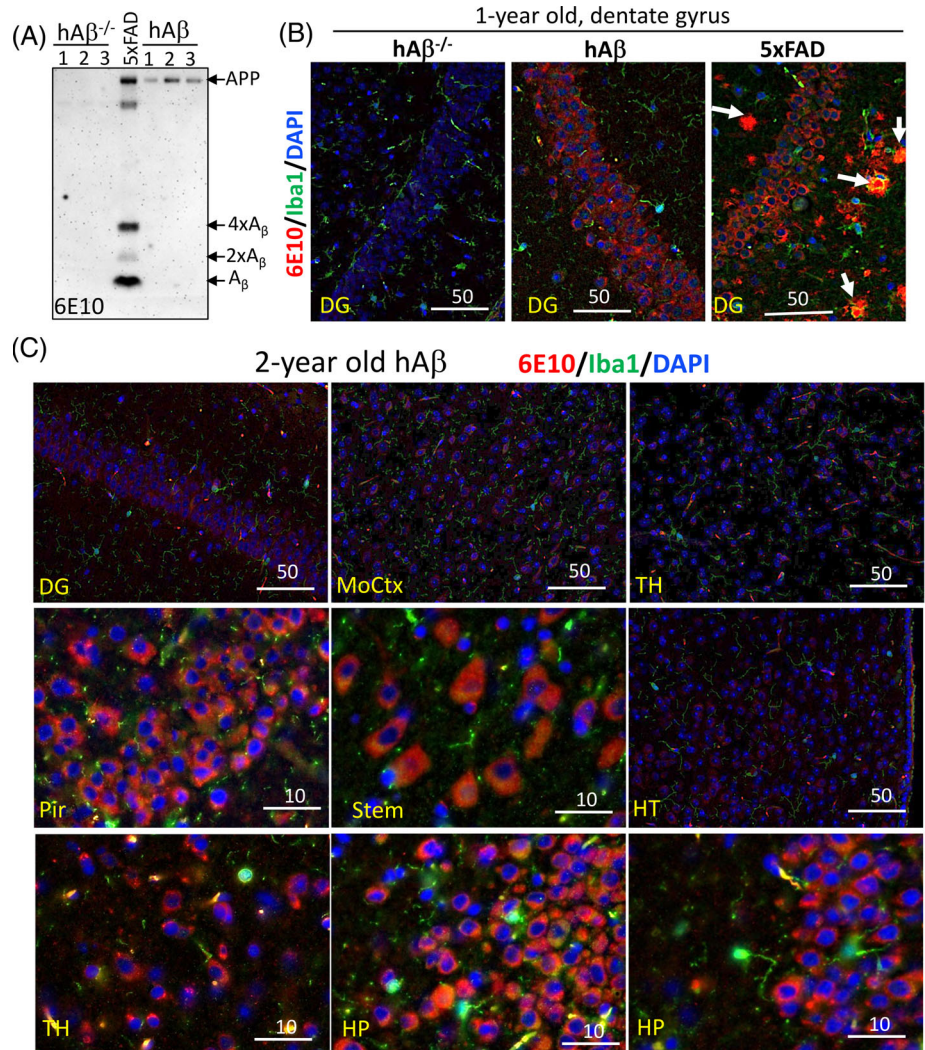
3.3 | HSV-1 does not induce A β pathology in hA β mice upon challenge via eye scarification

12-month-old male and female hA β mice were infected with 6.8×10^4 PFUs of the McKrae strain of HSV-1 via eye scarification. The survival curve for hA β mice aligned well with the curves observed for 5XFAD and B6SJL WT cohorts, suggesting that differences in genetic background including expression of APOE4 variant and R47H mutation of Trem2 in hA β mice did not change, profoundly, the host-pathogen interaction (Figure 1A). In animals that succumbed to acute herpes simplex encephalitis (HSE), piriform cortex, amygdala cortex and olfactory tubercle were consistently found to be infected with HSV-1, mirroring the pattern of viral spread seen in 5XFAD and WT (Figure 5A). To test whether HSV-1 triggered aggregation of A β , we systematically examined sections prepared across whole brains including areas with active replication of HSV-1 using co-immunostaining with 6E10 and a-HSV1 antibodies. 6E10 was used because it detects a range of aggregates including intracellular APP and A β , not just cores of A β plaques detectible by H31L21. Unfortunately, no evidence of A β aggregation was found even in the areas with active replication of the virus (Figure 5B). In fact, no differences in 6E10 immunoreactivity between HSV-1 infected and control groups could be detected (Figure 5D). Intracellular expression of APP was seen on large magnification images (Figure 5B). Consistent with our previous observations [38], Iba1-positive reactive myeloid cells, that engulf infected neurons, were found in sites of virus replication (Figure 5C).

3.4 | HSV-1 does not induce A β pathology in hA β mice upon intracranial challenge

Next, we decided to test whether HSV-1 administered directly into the brain via intracranial (IC) challenge triggers A β pathology in hA β mice. While IC inoculation is not physiological, delivering the virus directly to the cortex offers the most direct and effective way for establishing widespread acute HSV-1 infection in the CNS. 13-month-old male and female A β mice were inoculated IC with 2×10^3 or 10^3 PFUs/animal of McKrae. These doses were selected based on preliminary experiments to be close to the LD₅₀ dose. At both doses, 2×10^3 and 10^3 PFUs/animal, a fraction of animals succumbed to acute HSE, whereas 23% and 40%, respectively, survived the challenge showing the expected dose-dependence (Figure 6A). Staining with a-HSV1 and gD confirmed replication of HSV-1 in multiple brain areas including thalamus, hypothalamus, cortex and hippocampus of animals that succumbed to acute HSE (Figure 6B). However, careful examination throughout the whole brains of animals that succumbed to acute HSE did not reveal any A β pathology (Figure 6C). Animals that survived the challenge with 2×10^3 PFUs were examined at the days

FIGURE 4 Characterization of aged hA β mice. (A) Western blot of 1-year-old hA β mice ($n = 3$), control APOE4/Trem2**R47H* mice that express mouse APP (hA $\beta^{-/-}$, $n = 3$) and 5XFAD mouse used as a reference strain with 6E10. (B) Co-immunostaining of 1-year-old hA β ($n = 3$), hA $\beta^{-/-}$ ($n = 3$) and 5XFAD mice using 6E10 (red) and anti-Iba1 (green) antibodies. Expression of cellular APP with humanized A β segment is observed in hA β but not hA $\beta^{-/-}$ mice. Both hA β and hA $\beta^{-/-}$ lack extracellular A β aggregates that can be seen in 5XFAD mice. Arrows point at A β plaques in 5XFAD mice. (C) Co-immunostaining of 22- to 24-month-old hA β mice using 6E10 (red) and anti-Iba1 (green) antibodies ($n = 5$). While intracellular expression of APP can be seen in multiple brain regions, no A β plaques or extracellular A β aggregates can be found. DG, dentate gyrus; MoCtx, motor cortex; TH, thalamus; Pir, piriform cortex; HT, hypothalamus. Scale bars = 50 μ m in B and 50 and 10 μ m in C.



14 and 42 postinoculation. Consistent with previous studies [38], HSV-1 was not detectable in surviving animals, suggesting that active viral infection was resolved 2 weeks after direct IC challenge in the absence of A β pathology (Figure 6D). In fact, only cellular staining of APP could be observed (Figure 6C, D). Again, the animals that succumbed to acute HSE, surviving mice and controls showed no differences with respect to their 6E10 immunoreactivity (Figure 6E).

3.5 | HSV-1 does not induce A β pathology in hA β mice primed with LPS

Next, we decided to test whether an additional insult that induces neuroinflammation would help to trigger A β pathology in hA β mice challenged IC with HSV-1. LPS is known to induce chronic neuroinflammation and perturb A β homeostasis [39–41]. Previously, repeated intraperitoneal injections of LPS (0.25 mg/kg) resulted in neuroinflammation along with an increase in APP expression and accumulation of A β peptides in the hippocampus

and cortex [42]. In the current work, 13-month-old mice were injected intraperitoneally with LPS (1 mg/kg) once per week for six consecutive weeks and then infected IC with 2×10^3 PFUs of McKrae per animal a week after the last LPS treatment. The group challenged with McKrae showed a 20% survival rate (Figure 7A). No statistically significant difference with the group that received the same dose of McKrae in the absence of LPS priming can be observed (Figure 7A), suggesting that priming with LPS did not significantly affect the susceptibility of the animals to the virus. Careful examination of animals primed with LPS that succumbed to acute infection revealed that HSV-1 infection in multiple brain areas including motor and auditory cortices, thalamus, and hypothalamus, however, there was an absence of A β pathology (Figure 7B). Two control hA β groups were examined: one was treated with LPS for 6 weeks then inoculated IC with PBS instead of HSV-1, and another was injected with PBS for 6 weeks instead of LPS (Figure 7C,D). Both control groups were HSV-1 negative and did not show any A β pathology (Figure 7D). Quantitative analysis of 6E10 immunoreactivity showed no

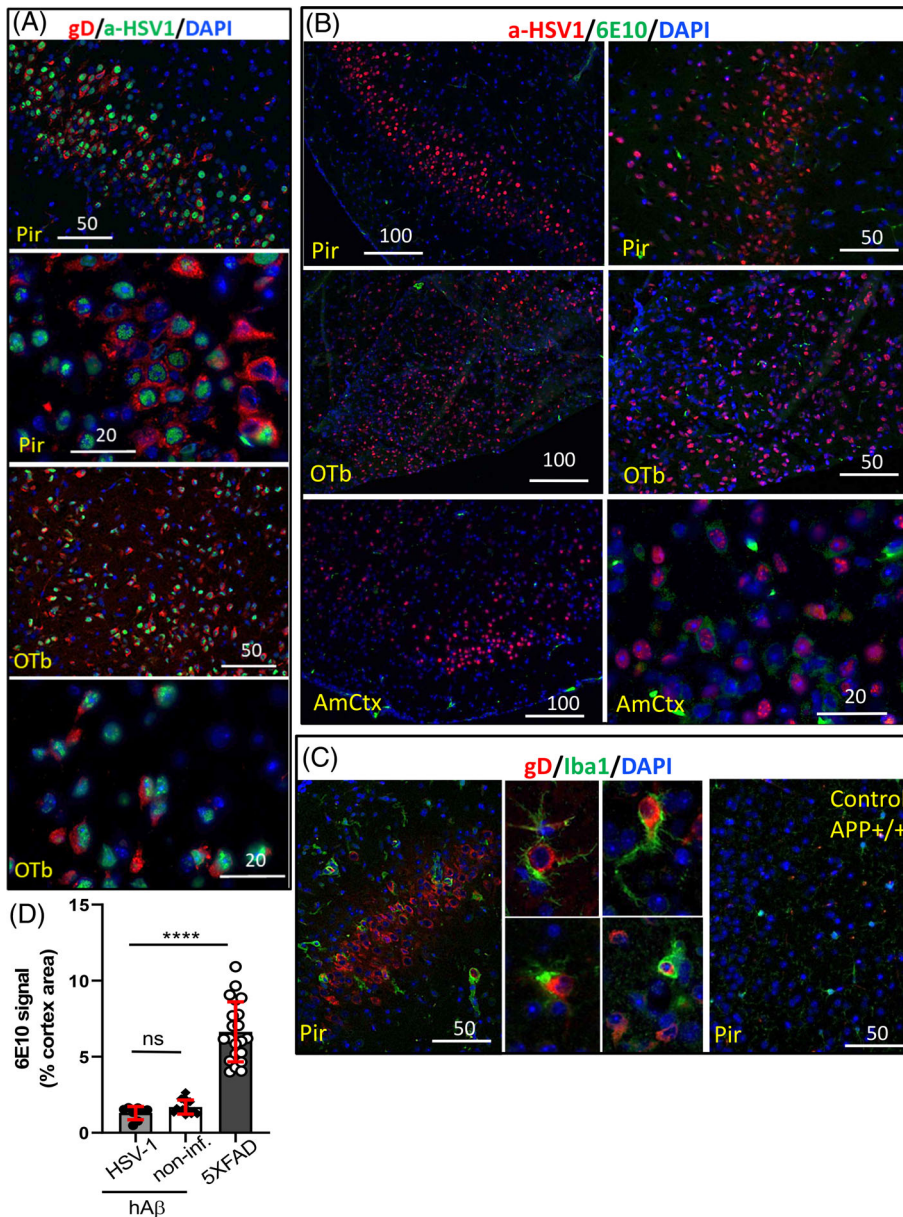


FIGURE 5 Upon challenge of hA β mice via eye scarification, HSV-1 replicates in a brain but does not induce A β pathology. 12-month-old hA β mice were infected with 6.8×10^4 PFUs McKrae strain of HSV-1 via eye scarification and examined 160–230 h postchallenge using co-immunostaining for HSV-1 replication centers (a-HSV1 antibody, green) and gD (anti-gD antibody, red), $n = 6$ (A); for A β aggregates (6E10 antibody, green) and HSV-1 virus (a-HSV1 antibody, red), $n = 6$ (B), or for myeloid cells (anti-Iba1 antibody, green) and gD (anti-gD antibody, red), $n = 2$ (C). Noninfected, age-matched hA β control stained with anti-Iba1 and anti-gD antibodies is shown in C. Nuclei stained with DAPI (blue). Pir, piriform cortex; OTb, olfactory tubercle; AmCtx, amygdala cortex. Scale bars = 20, 50 or 100 μ m. (D) Quantification of percent area covered by 6E10 signal in cortex of hA β mice infected with HSV-1 ($n = 3$), noninfected hA β mice and noninfected 12-month old 5XFAD mice ($n = 4$) provided as references [8–22] fields of view were analyzed for each group. Data expressed as mean \pm SD, unpaired parametric two-tailed t-test was used, **** $p < 0.0001$, ns = not statistically significant.

differences between the experimental and control groups (Figure 7C).

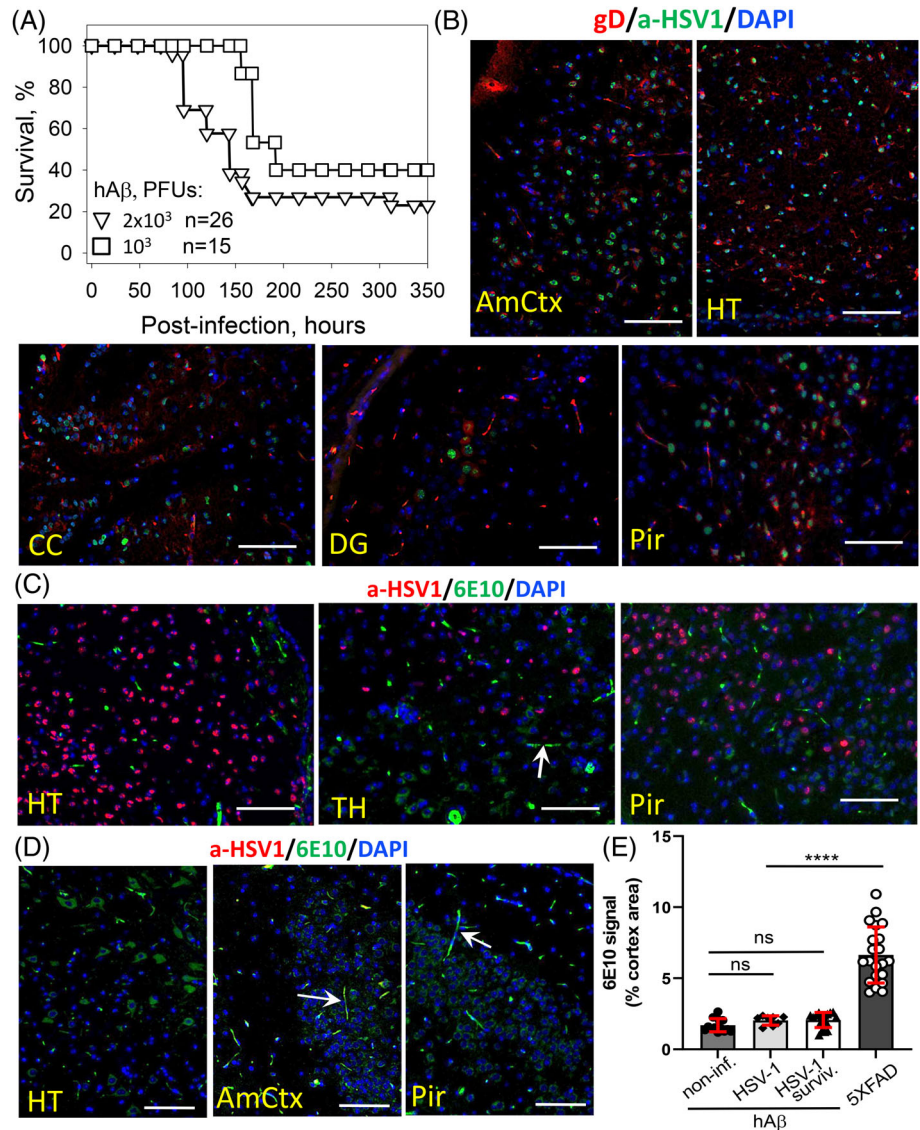
3.6 | HSV-1 does not induce A β pathology in hA β mice challenged IC with high doses of McKrae or 17syn+

Finally, we tested whether A β pathology could be induced by the highest dose of HSV-1 that we can generate in Vero cells. 13-month-old male and female hA β mice were challenged IC with 10^6 PFUs per animal of McKrae. In addition, to examine whether strain-specific features are important, a separate cohort of hA β mice were challenged with 10^6 PFUs of the 17syn+ strain of HSV-1 per animal. Considering that 1 PFU consists of 50–200 viral particles [43] and that a mouse brain has

approximately 70×10^6 neurons, the dose 10^6 PFUs delivers one viral particle per neuronal cell, on average.

hA β mice challenged with McKrae induced very aggressive acute HSE with short incubation times and 100% death rate, whereas the cohort challenged with 17syn+ displayed a longer incubation time and partial survival (Figure 8A). These results are consistent with the previous studies, demonstrating that McKrae is more neurovirulent than the 17syn+ strain [44, 45]. In mice that succumbed to acute HSE upon inoculation with McKrae or 17syn+, multiple brain areas including thalamus, hypothalamus, hippocampus and cortex were affected and showed replication of HSV-1 (Figure 8B). However, no A β pathology could be found in brain regions regardless of whether or not they were affected by HSV-1 (Figure 8B). No differences in 6E10 immunoreactivity between controls and the groups that

FIGURE 6 HSV-1 does not induce A β pathology in hA β mice upon intracranial challenge. (A) Survival curves for 13-month-old hA β mice challenged IC with 2×10^3 PFUs (triangles) or 10^3 PFUs (squares) of McKrae strain per mouse. (B) Co-immunostaining for HSV-1 replication centers (a-HSV1 antibody, green) and gD (anti-gD antibody, red) along with nuclei (DAPI, blue) in 13-month-old hA β mice ($n = 17$) that succumbed to acute HSE. (C) Co-immunostaining of 13-month-old hA β using 6E10 (green) and a-HSV1 (red) antibodies along with nuclei (DAPI, blue). (D) Co-immunostaining for HSV-1 replication centers (a-HSV1 antibody, green) and 6E10 (green) along with nuclei (DAPI, blue) in 13-month-old hA β mice ($n = 6$) that survived IC challenge. In B and C, animals were examined at 96–200 h postinfection. In D, animals were examined at 42 days postinfection. AmCtx, amygdala cortex; HT, hypothalamus; CC, corpus callosum; DG, dentate gyrus; TH, thalamus; Pir, piriform cortex; Arrows point at staining of blood vessels. Scale bars = 50 μ m. (E) Quantification of percent area covered by 6E10 signal in cortex of noninfected hA β mice ($n = 5$), hA β mice infected with 2×10^3 PFUs of McKrae that succumbed to acute HSE ($n = 4$) or survived HSV-1 challenge and examined at 42 days postinfection ($n = 4$), or noninfected 12-month old 5XFAD mice ($n = 4$) provided as references [8–21] fields of view were analyzed for each group. Data expressed as mean \pm SD, unpaired parametric two-tailed t-test was used, **** $p < 0.0001$, ns = not statistically significant.



succumbed to acute HSE after McKrae or 17syn+ challenges could be detected (Figure 8D). Animals that survived the challenge upon infection with 17syn+ strain were examined at 2 weeks postinfection. No active replication sites or A β pathology could be found in surviving animals (Figure 8C).

In human and mouse brains, myeloid cells are responsible for recognizing, engulfing and phagocytosing of neurons infected with herpes viruses [46]. Indeed, co-immunostaining of animals that succumb to acute HSE using gD and anti-Iba1 antibodies revealed reactive microglia/macrophages engulfing HSV-1-infected neurons (Figures S1 and S2). Along with Iba1-positive cells, activated GFAP-positive astrocytes were also present in close proximity to infected cells, however, did not participate in engulfing neuronal bodies (Figure S1). Instead, processes of activated astrocytes were frequently found in close contact with infected neurons, suggesting that the response to infection was coordinated between myeloid cells and astrocytes (Figure S1).

3.7 | HSV-1 infects APP-positive and APP-negative neurons

For testing whether neuronal cells expressing APP are protected from HSV-1 infection, cellular APP expression was examined in cells with active replication of HSV-1. Both confocal and widefield microscopy imaging found viral replication centers in both APP-positive and APP-negative cells (Figure 9A, Figure S3). To test whether the cellular levels of APP and A β peptides change in APP-positive cells in response to infection, the intensity of staining with 6E10 was quantified in individual cells infected with the virus and compared with 6E10 intensities in noninfected, age-matched hA β mice (Figure 9B). APP-positive cells infected with HSV-1 were identified using a-HSV1 antibodies (Figure 9A). To validate this approach, cellular levels of APP/A β were also quantified in noninfected 5XFAD mice, which express APP at higher levels relative to hA β mice (Figure 4A). As expected, in individual cells of 5XFAD mice, the levels of

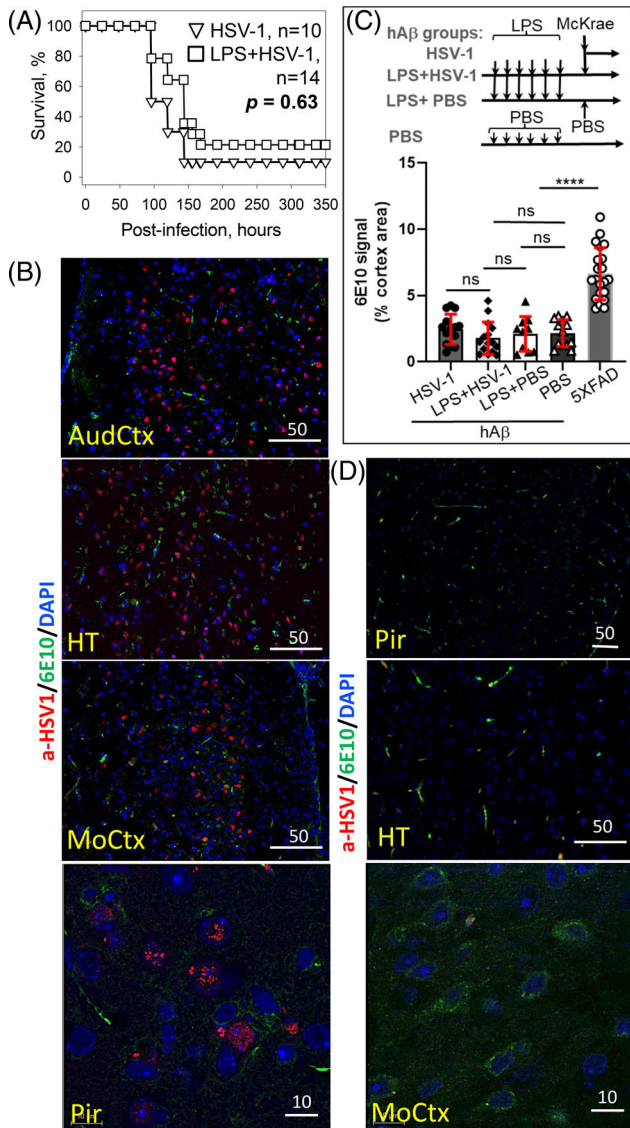


FIGURE 7 HSV-1 does not induce A β pathology in hA β mice primed with LPS. (A) Survival curves for 13-month-old hA β that were challenged IC with 2×10^3 PFUs of McKrae strain per mouse or injected IP with LPS once per week for 6 consecutive weeks and then challenged IC with McKrae. Statistical significance (p) was calculated using the log-rank (Mantel-Cox) test. (B) Co-immunostaining of hA β mice that were primed with LPS, challenged with 2×10^3 PFUs of McKrae and succumbed to acute HSE using 6E10 (green) and a-HSV1 (red) antibodies along with nuclei (DAPI, blue) ($n = 6$). (C) Schematic diagram illustrating experimental and control hA β groups, and quantification of percent area covered by 6E10 signal in cortex of mice of the following groups: HSV-1, hA β mice challenged with 2×10^3 PFUs of McKrae ($n = 3$); LPS + HSV-1, hA β mice treated with LPS, then challenged with 2×10^3 PFUs of McKrae and succumbed to acute HSE ($n = 3$); LPS + PBS, hA β mice treated with LPS, then inoculated IC with PBS ($n = 3$); PBS, hA β mice inoculated with PBS for 6 weeks instead of LPS ($n = 3$). Quantification in noninfected 12-month old 5XFAD mice ($n = 4$) provided as references [10–22] fields of view were analyzed for each group. Data expressed as mean \pm SD, unpaired parametric two-tailed t -test was used, **** $p < 0.0001$, ns = not statistically significant. (D) Co-immunostaining of 13-month-old LPS + PBS hA β control group using 6E10 (green) and a-HSV1 (red) antibodies along with nuclei (DAPI, blue) ($n = 5$). AudCtx, auditory cortex; HT, hypothalamus; MoCtx, motor cortex; Pir, piriform cortex. Arrows point at staining of blood vessels. Scale bars = 50 and 10 μ m.

APP/A β were higher relative to the cellular levels in non-infected hA β mice (Figure 9B). However, in HSV-1-infected cells of hA β mice, the levels of APP/A β did not differ from the APP/A β levels in noninfected hA β mice (Figure 9B).

3.8 | hA β mouse model is susceptible to chronic neurodegeneration

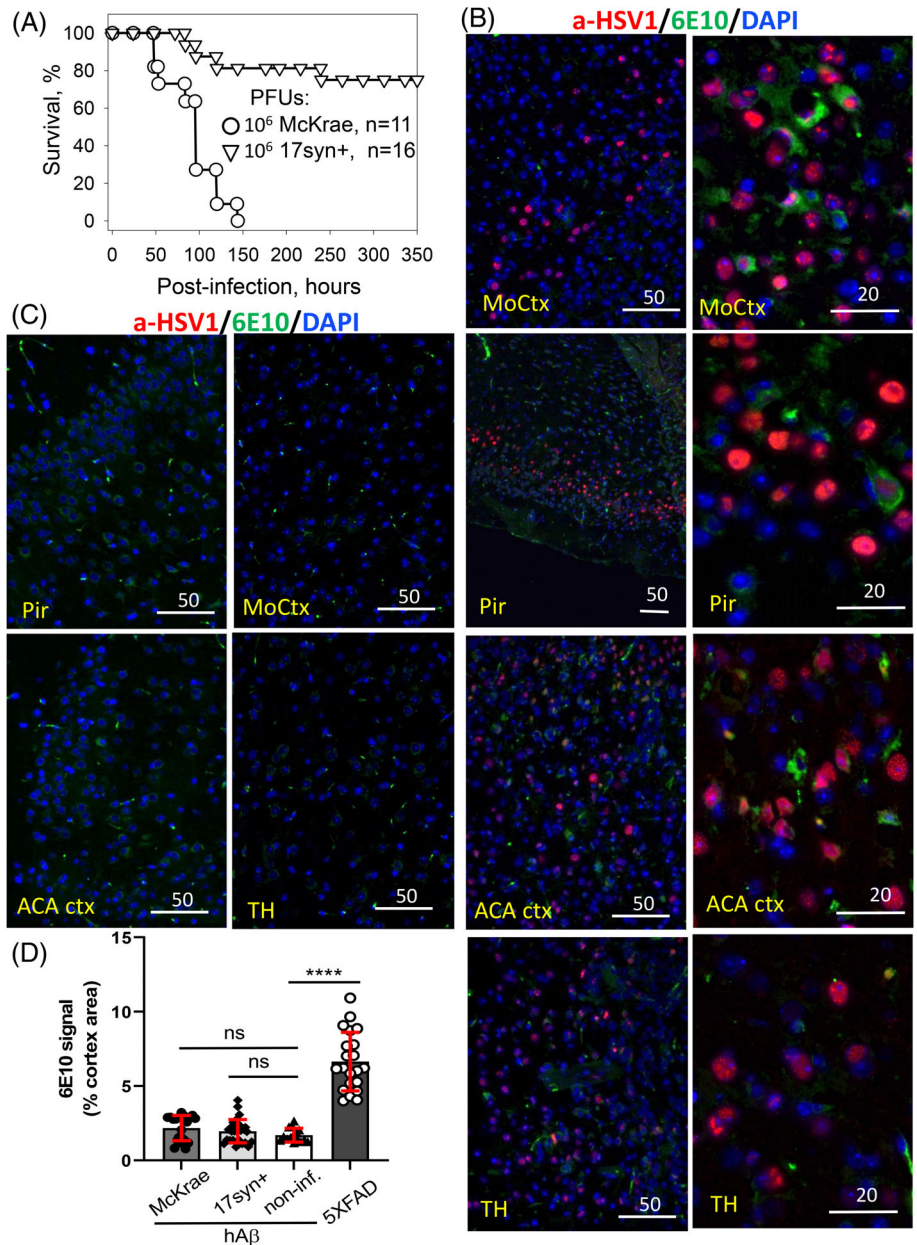
As our experiments with HSV-1 progressed, it became evident that in hA β mice, Trem2* $R47H$ is expressed at approximately 50% of the normal expression level of Trem2. The reduced expression level has been traced to aberrant splicing of the mutant mouse allele [47]. Low expression of TREM2* $R47H$ raised concerns regarding the possible limited susceptibility of the hA β mouse model to chronic neurodegeneration and, specifically, a deficiency in the phagocytic activity of microglia. To mitigate this concern, hA β mice were infected with prions via the intraperitoneal route (Figure 10). The time course of the disease in hA β mice was very similar to that of C57Bl.6J mice infected using the same dose, prion strain, and route of infection (Figure 10C). The disease progressed slightly faster in hA β mice relative to C57Bl.6 J, yet the difference in incubation times was borderline statistically significant. This result suggests that the Trem2* $R47H$ variant, its low expression level, or humanized APOE4 variant, do not substantially affect the prion disease pathogenesis. Similar to the prion-infected C57Bl.6 J mice [31], highly reactive Iba1-positive myeloid cells of amoeboid shape with intracellular PrP^{Sc} aggregates were observed in prion-infected hA β mice at the preclinical stage of the disease, suggesting that Iba1-positive myeloid cells maintained phagocytic activity toward PrP^{Sc} (Figure 10A). Moreover, prion-infected hA β mice also displayed intensive engulfment of neuronal cells by Iba1-positive myeloid cells, mirroring the same neuronal engulfment seen in C57Bl.6 J mice (Figure 10B) [48]. Together, these results illustrate the susceptibility in the hA β model to chronic neurodegeneration and preservation of phagocytic activity by the Iba1-positive myeloid population.

3.9 | In response to acute infection, peripheral myeloid cells infiltrate brain parenchyma and phagocytose HSV-1-infected neurons

The lack of A β aggregation in response to viral infection, the lack of changes in cellular levels of APP/A β in hA β mice, as well as lack of any protective effect of APP overexpression and A β plaques in young and aged 5XFAD mice [38], respectively, argue against the hypothesis on the protective role of A β . To get insight into the mechanisms that defend the CNS against acute HSE, we performed flow cytometry analysis of brain tissues from hA β

FIGURE 8 HSV-1 does not induce A β pathology in hA β mice upon intracranial challenge with high viral doses.

(A) Survival curves for 13-month-old hA β mice challenged IC with 10^6 PFUs per mouse of McKrae (circles) or 17syn + strain (triangles). (B) Co-immunostaining for HSV-1 replication centers (a-HSV1 antibody, red) and 6E10 antibody (red) along with nuclei (DAPI, blue) in 13-month-old hA β mice ($n = 9$) that succumbed to acute HSE upon challenge with 10^6 PFUs of McKrae. (C) Co-immunostaining for HSV-1 replication centers (a-HSV1 antibody, red) and 6E10 antibody (green) along with nuclei (DAPI, blue) in 13-month-old hA β mice that survived challenge with 10^6 PFUs of 17syn + ($n = 5$). Animals were examined at 336 h postinfection. MoCtx, motor cortex; Pir, piriform cortex; ACA Ctx, anterior cingulate area cortex; TH, thalamus. Scale bars = 20 or 50 μ m. (D) Quantification of percent area covered by 6E10 signal in cortex of hA β mice infected with McKrae ($n = 6$) or 17Syn + ($n = 3$) that succumbed to acute HSE, noninfected hA β mice ($n = 5$), or noninfected 12-month old 5XFAD mice ($n = 4$) provided as references [14–27] fields of view were analyzed for each group. Data expressed as mean \pm SD, unpaired parametric two-tailed t-test was used, **** $p < 0.0001$, ns = not statistically significant.



mice challenged IC with McKrae. CD45, CD11b and Ly6C markers were used to identify populations of resident microglia (MG, CD45^{int}CD11b⁺Ly6C⁻) and infiltrating myeloid cells (iMy, CD45^{hi}CD11b⁺Ly6C⁺) and lymphocytes (iLym, CD45^{hi}CD11b⁻). At 72 h postinfection, the infiltrating leukocyte populations increased on average by 91- and 14.7-fold, respectively, whereas resident microglia showed only a statistically insignificant upward trend (Figure 11A, B). Co-localization of the phagocytic marker CD68 and the neuron-specific marker NeuN with specific cell types established that in their homeostatic state, resident microglia express a basal phagocytic activity, which trended upward upon infection (Figure 11C, D). Similarly, an upward trend in phagocytic activity of microglia was also seen in phagocytic assays that employed 0.5 or 1.0 μ m fluorescent beads (Figure 11E–G). While these data are

consistent with previous results that resident microglia take part in the phagocytosis of neuronal cells, mild upregulation of phagocytic activity suggests that microglia might not constitute the primary defense mechanism against HSV-1 infection, at least within the first 72 h postinfection. Unexpectedly, a significant fraction of peripheral infiltrating myeloid cells displayed CD68 marker and incorporated NeuN protein documenting the phagocytic phenotype of infiltrating myeloid cells (Figure 11B). The ex vivo phagocytic assay with beads confirmed that a considerable fraction of infiltrating myeloid cells that responded to infection were phagocytically active (Figure 11E–G). When multiplied by a multiple-fold growth in the population of infiltrating myeloid cells attracted to the infection sites, phagocytic activity of infiltrating myeloid cells appears to represent the primary defense mechanism against HSV-1.

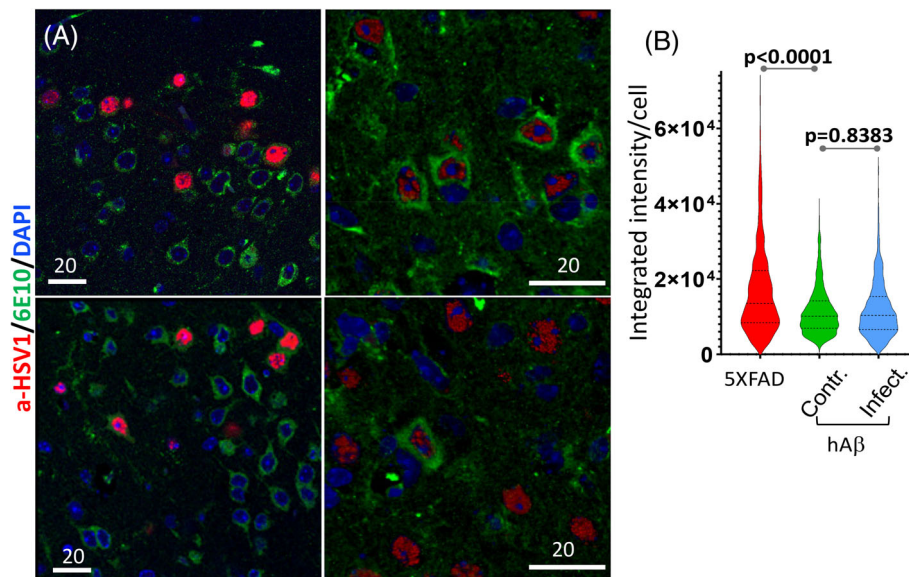


FIGURE 9 HSV-1 infects APP-positive and APP-negative neurons. (A) 13-month-old hA β that succumbed to HSE upon IC challenge with 2×10^3 PFUs of McKrae were co-immunostained for APP/A β (6E10 antibody, green) and HSV-1 replication centers (a-HSV1 antibodies, red) along with nuclei (DAPI, blue) and examined using confocal microscopy. Scale bars = 20 μ m. (B) Quantification of intracellular APP/A β levels using staining with 6E10 antibody in individual HSV-1-infected cells in 13-month-old hA β mice that succumbed to acute HSE ($n = 3$, 447 cells) and in noninfected age-matched control hA β mice ($n = 3$, 1499 cells). Quantification of intracellular APP/A β levels in noninfected, age-matched 5XFAD ($n = 3$, 519 cells) is provided as reference. The dashed lines in violone plots show the median and quartiles. P is calculated using an unpaired nonparametric two-tailed Mann–Whitney U test.

To confirm these results, brains of hA β mice challenged IC with McKrae were examined using immunostaining for Galectin 3 (Gal3, also known as MAC2 or LGALS3). Gal3 was recently shown to be a specific, long-lasting marker of infiltrating myeloid cells [49]. Coimmunostaining using anti-Gal3 and a-HSV1 antibodies revealed massive infiltration by Gal3-positive cells into brain areas affected by the virus (Figure 12A). Individual HSV-1-infected cells were engulfed or surrounded by multiple Gal3-positive cells of ameboid shape (Figure 12A, panels 2 and 3). This pattern was different from the phagocytosis by Iba1-positive resident microglia, where infected neurons were engulfed by individual microglial cells with partially ramified morphology and long processes (Figure 5C).

Co-immunostaining with anti-Gal3 and anti-Iba1 antibodies revealed that most of the Gal3-positive cells were Iba1-negative (Figure 12B, panes 1, 2, 4) and, vice versa, most of the Iba1-positive cells were Gal3-negative (Figure 12B, panes 1, 2, 4). A fraction of Gal3-positive cells displayed Iba1 immunoreactivity on the cell periphery (Figure 12B, panes 5, 6), a pattern of Iba1 staining different from that seen for resident microglia. These results suggest that the majority of peripheral myeloid cells did not express the Iba1 marker at least within the time frame of this experiment. We do not know whether the peripheral localization of Iba1 in Gal3-positive cells was due to close contact with resident microglia or endogenous expression of Iba1 in a fraction of infiltrating Gal3-positive cells. Nevertheless, staining with Gal3

confirmed massive infiltration of peripheral myeloid cells to the sites of HSV-1 infection along with seclusion and phagocytosis of infected cells by infiltrating Gal3-positive myeloid cells.

4 | DISCUSSION

According to the amyloid cascade hypothesis, deposition of A β peptides in the form of A β plaques or aggregates is the first key step that triggers a cascade of pathological events including neuroinflammation and formation of the paired helical filaments of tau that lead to Alzheimer's disease [3]. The pathogen hypothesis proposed that aggregation of A β peptides is triggered by pathogens and serves as a protective mechanism in response to infection of the CNS [7–10]. Herpesviruses emerged as leading pathogens linked to AD [4–7, 14, 50, 51]. The current study aimed at testing a causative relationship between HSV-1 infection of the CNS and A β pathology. The current work focuses exclusively on A β pathology, because pathogens are expected to trigger A β aggregation directly as stipulated by the pathogen hypothesis and because A β aggregation is considered to be one of the first events leading toward AD.

Aged 5XFAD mice were employed to test whether A β plaques have protective effects against HSV-1 infection introduced via a physiological route. At young age, 5XFADs show sex-specific differences in cerebral levels of A β peptides [35], however, by 14 months of age both

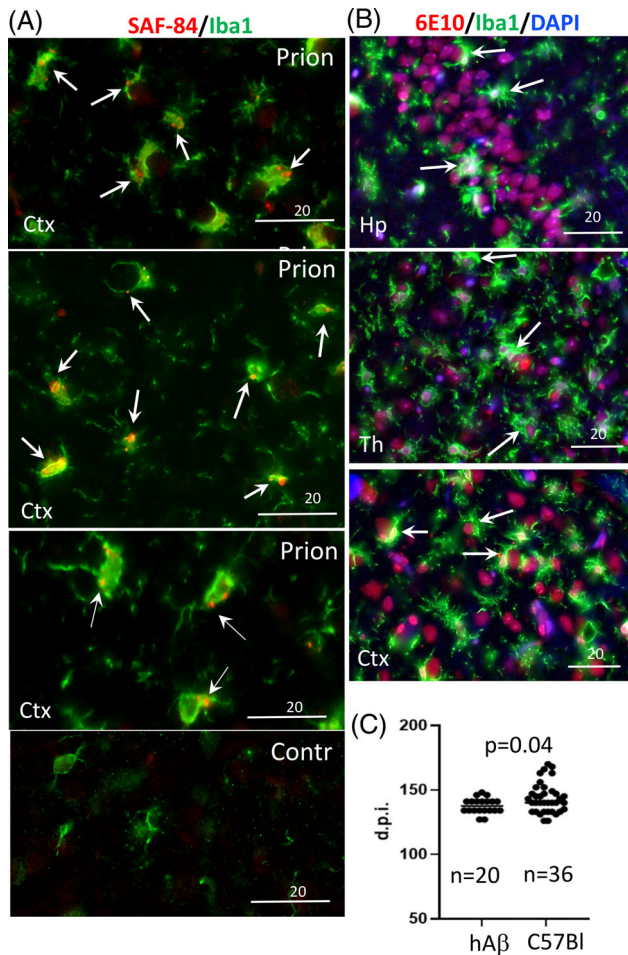


FIGURE 10 hA β mice are susceptible to prion disease. hA β and C57Bl.6J female and male mice were infected with the SSLOW prion strain via the intraperitoneal route. (A) Co-immunostaining of presymptomatic hA β mice at 115 days postinfection with SSLOW and age-matched controls for microglia (anti-Iba1 antibody, green) and PrP^{Sc} (SAF-84 antibody, red). Arrows point at PrP^{Sc} deposits colocalized with microglia. (B) Co-immunostaining of terminal hA β mice infected with SSLOW for microglia (anti-Iba1 antibody, green) and APP (6E10 antibody, red). Arrows point at reactive microglia engulfing neurons. Hp, hippocampus; Ctx, cortex. Scale bars = 20 μ m. (C) Incubation time to terminal diseases in hA β and C57Bl.6J mice inoculated with 1% SSLOW brain homogenate via the intraperitoneal route. The groups were compared by Student's unpaired *t* test.

male and female display abundant widespread A β plaques. In 14-month-old 5XFAD mice infected via eye scarification, high density of A β aggregates did not improve survival time or rate of survival relative to the age-matched WT littermates. In aged 5XFAD mice, HSV-1 spread to the brain and affected the same brain areas as in WT littermates suggesting that A β aggregates do not affect host-pathogen interaction. Moreover, in 5XFAD mice, viral replication sites were seen in brain areas with a high density of extracellular A β deposits, however, no association between HSV-1 and A β aggregates could be found. These results are in agreement with our previous studies illustrating that (i) HSV-1 fails to induce A β aggregation in young 5XFAD mice, (ii) the

virus does not bind to A β aggregates in aged 5XFAD mice, and (iii) regardless of animal age, the 5XFAD genotype does not protect against HSV-1 administered via the intracranial route [38]. Our previous and current results contradict the studies where HSV-1 colocalized with A β plaques in 5XFAD mice challenged via IC route with a very high dose of HSV-1 (2×10^7 PFUs per brain) of an unspecified strain identity [7]. In a mouse brain, the viral load of 2×10^7 PFUs delivers more than 10 viral particles per 1 neuronal cell, on average. It is unlikely that either organism, mouse or human, would encounter such a high dose of HSV-1 during their lifetime. Moreover, in the absence of quantification, it is not clear whether the apparent colocalization with plaques was due to preferential affinity of HSV-1 to A β or simply overloading the brain with a high viral dose. Lack of association between pre-formed A β aggregates and HSV-1 in the current work supports the hypothesis that A β aggregates do not entrap the virus in vivo nor do they interfere with its spread to the CNS upon infection via a physiological route.

While 5XFAD mice exhibit widespread A β pathology and neuroinflammation, concerns have been raised regarding the physiological relevance of this mouse model. First, in 5XFAD, APP combines several familial AD-associated mutations (Swedish K670N and M671L, Florida I716V, and London V717I). Second, APP expression exceeds significantly its endogenous expression level and, third, it is expressed under the Thy1 promoter [35]. Moreover, A β pathology that develops spontaneously starting at 2 months of age [35], poses limitations for testing a causative relationship between pathogens and A β plaques. To test whether HSV-1 triggers A β pathology in a more relevant setting, we used the hA β mouse model that expresses APP under an endogenous mouse promoter. hA β mice also express high-risk variants of *APOE* and *Trem2* genes, which significantly increase the risk, yet are not sufficient to cause late-onset AD at a 100% rate. Studies using *APOE* knockout (KO), or humanized *APOE3/APOE4* transgenic mice revealed that neuroinvasion and spread of HSV-1 in a brain is significantly facilitated in *APOE4* mice in comparison to *APOE* knock out or *APOE3* mice [52–55]. In humans, conflicting results have been reported on whether infection with HSV-1 represents an additional risk for AD in individuals with the *APOE4* genotype [56, 57]. Nevertheless, we hypothesized that the genetic risk factors attributed to *APOE4* and *Trem2* R47H could be amplified by a risk related to viral infection of the CNS. Moreover, previous studies revealed that *APOE4* exacerbates A β pathology via enhancing amyloid deposition during the early stages of A β aggregation [29, 30]. We chose to use 13-month-old animals to avoid confounding effects due to natural death, which is noticeable at approximately 16 months of age.

The current study is the first to examine aged hA β (hA β /A β 4/Trem2*R47H) mice. As expected, neuronal

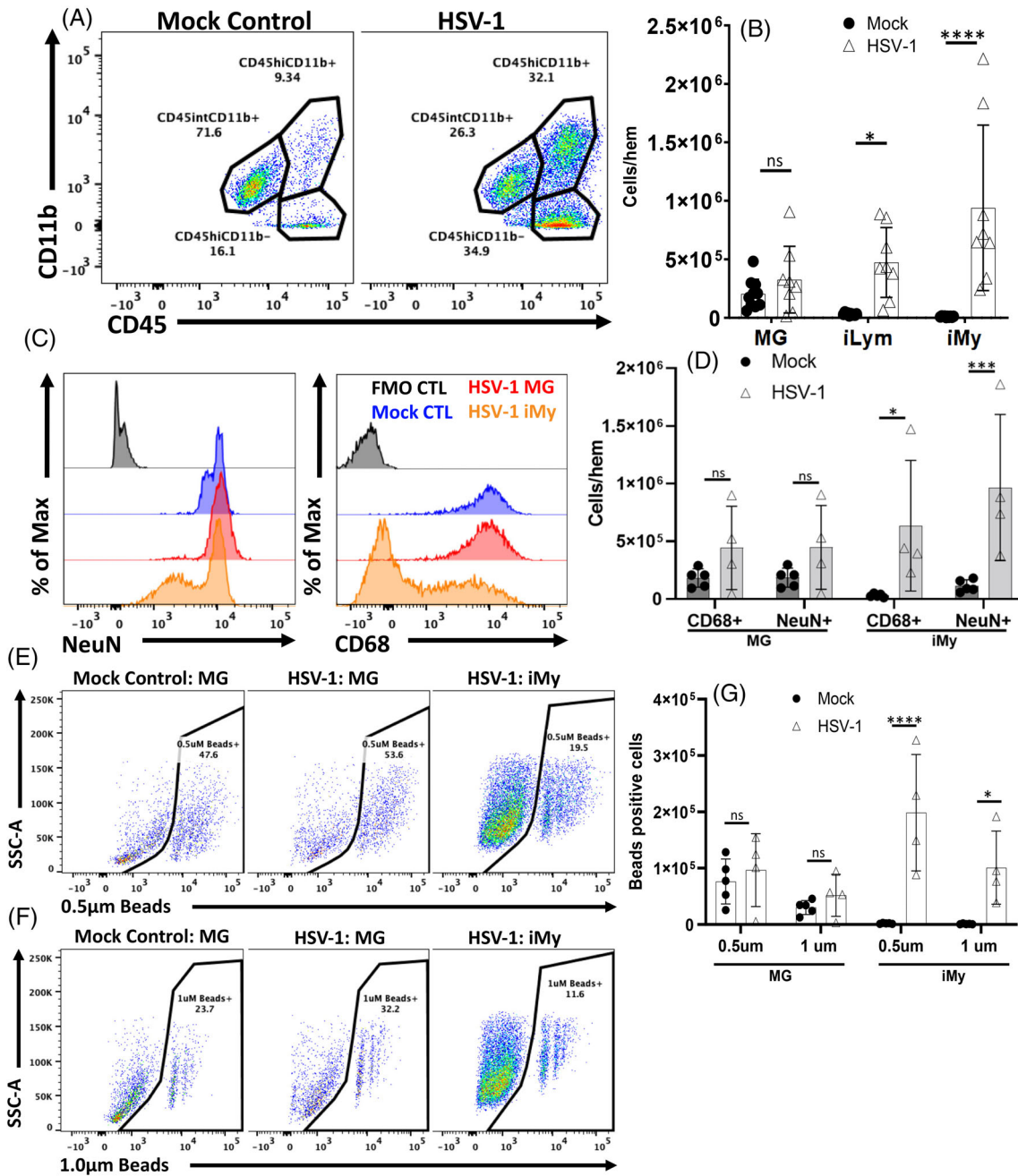
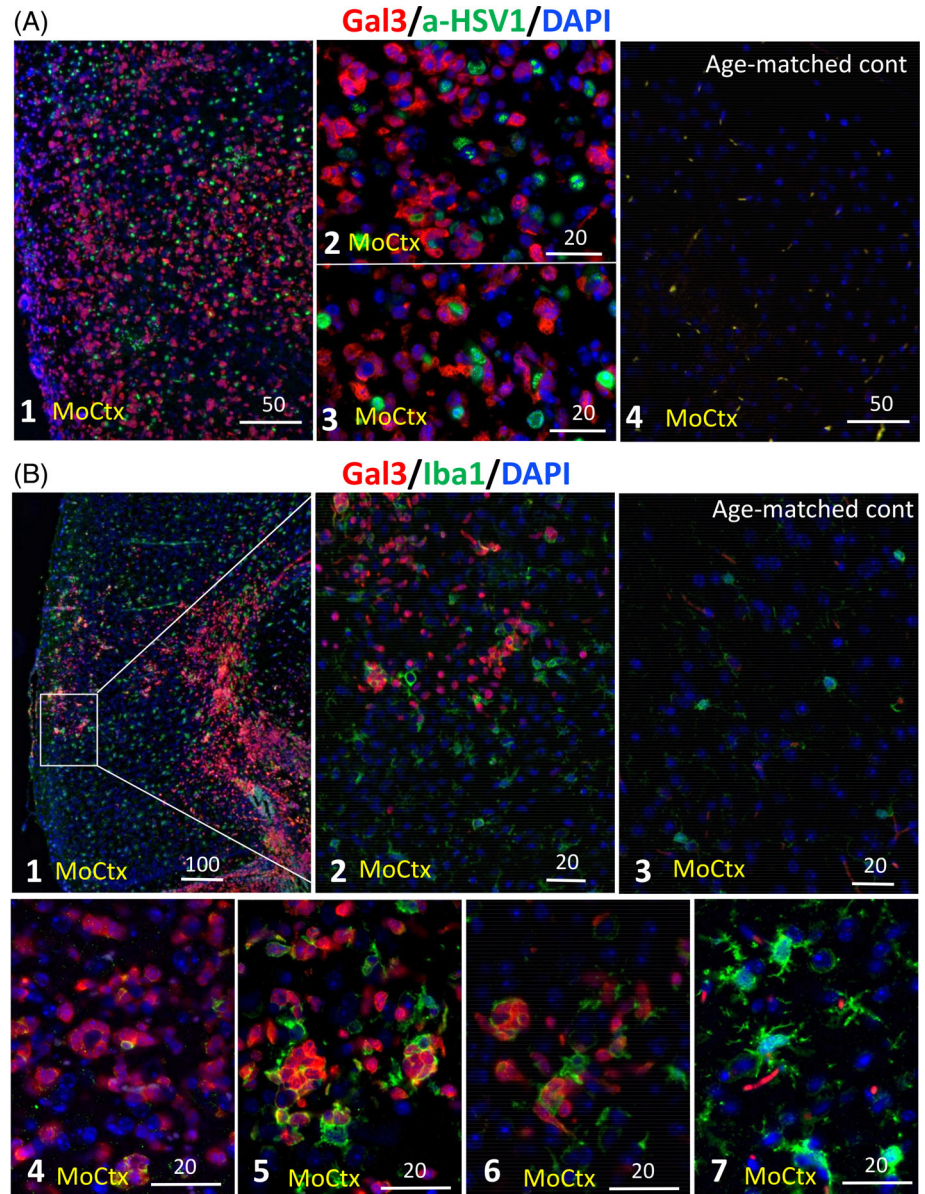


FIGURE 11 Flow cytometry analysis of resident and infiltrating myeloid cells and their phagocytic activity. 13-month-old hA β mice were challenged IC with 10^6 PFUs of McKrae per mouse or mock inoculum (Mock CNL) and analyzed by flow cytometry at 72 h postinfection. (A) Representative dot plots show the relative composition of brain-resident microglia (MG, CD45^{int}CD11b⁺Ly6C⁻), infiltrating lymphocytes (iLym, CD45^{hi}CD11b⁻), and infiltrating myeloid cells (iMy, CD45^{hi}CD11b⁺) in control and infected mice. (B) The number of each cell population per hemisphere for each group is quantified. (C) Representative histograms depict the relative intensity level of the neuronal antigen, NeuN, and the phagocytic marker, CD68, inside mock control (*in blue*) and HSV-1 (*in red*) microglia and infiltrating myeloid cells (*in orange*). (D) The number of NeuN-positive and CD68-positive phagocytic myeloid cells per hemisphere is quantified. Representative dot plots illustrate the percentage of microglia and infiltrating myeloid cells that engulfed (E) 0.5 μ m and (F) 1.0 μ m fluorescent latex beads at 72 h postinfection. (G) The total number of bead-positive phagocytes in each group is quantified. For panel B, data were combined from two independent experiments. For all experiments, the number of animals were 4–5 per group. For all histograms, fluorescence minus one (FMO) controls are shown in gray. CTL, control; hi, high; HSV-1, herpes simplex virus-1; iMy, infiltrating myeloid cells; iLym, infiltrating lymphocytes; int, intermediate; MG, microglia; Max, Maximum; ns, not significant; SSC-A, side scatter-area. Data expressed as mean \pm SEM. Data were analyzed using two-way ANNOVA with Sidak’s multiple comparison test, with individual variances computed for each comparison and expressed as mean \pm SD (* p < 0.05, *** p < 0.0005, and **** p < 0.00005).

APP expression was seen in multiple brain regions including the hippocampus, cortex, thalamus, hypothalamus and stem, although at levels significantly lower relative to

APP expression in 5XFADs. Like the majority of the human population, aged hA β mice that lived up to 24 months in our colony showed no obvious signs of A β

FIGURE 12 Infiltration of Gal3-positive cells in the infection sites of hA β mice during acute HSE. 13-month-old hA β mice were challenged IC with 2×10^3 PFUs of McKrae per mouse. Mice that succumbed to HSE 96–200 h postinfection were analyzed using co-immunostaining with anti-Gal3 (red) and a-HSV1 (green) antibodies $n = 9$ (A), or anti-Gal3 (red) and anti-Iba1 (green) antibodies $n = 9$ (B). In A, panel 2 shows field of view different from panels 1 and 3. Panel 4 in A and panel 3 in B show co-immunostaining of mock age-matched controls. MoCtx, motor cortex. Scale bars = 20, 50, or 100 μ m.



pathology or neuroinflammation, illustrating that this mouse line does not develop A β plaques spontaneously. Recent transcriptome studies of similar mouse model that expresses two risk variants, APOE4 and Trem2*R47H, identified age-dependent molecular changes in multiple pathways that overlapped with AD-associated pathways in human [58]. Nevertheless, lack of amyloid pathology at old age in hA β mice suggests these mice offer a sensitized baseline model for testing risks associated with viral infections or other environmental insults in the context of normal aging combined with genetic AD risk factors.

To test whether HSV-1 triggers A β pathology in hA β mice, several experiments were performed where 13-month-old hA β mice were infected with HSV-1 via (i) eye scarification with McKrae, (ii) IC inoculation with McKrae, (iii) IC inoculation with McKrae after priming with LPS for 6 weeks, or (iv) IC inoculation with high

doses of McKrae or 17syn+ strains. Two HSV-1 strains were tested, because strain-specific differences dictate a number of features of host-pathogen interaction including neurovirulence [44, 59–61]. In all experimental groups including the cohort infected via eye scarification, active replication of HSV-1 was confirmed in animal brains using immunostaining with antibodies toward viral replication centers and the envelope protein gD, which were validated in a series of positive and negative controls in our current and previous studies [38]. Brains of hA β mice that succumbed to acute HSE and those that survived the challenges were carefully examined. No signs of A β aggregation could be found in mice that succumbed to HSE or survived in any of the experimental groups. HSV-1 was found in brain areas expressing APP, suggesting that physiological levels of APP do not prevent viral spread. Moreover, HSV-1 transcription centers were

found in cells whether they expressed APP or not. Cells that were infected with HSV-1 showed no changes in amounts of APP/A β in response to the infection, as quantified using staining with 6E10 antibody and confocal microscopy. These results argue that HSV-1 does not trigger A β pathology in mice and that APP, when expressed under an endogenous promoter, does not affect host-pathogen interactions.

Together with several recent studies [38, 62, 63], our work raises serious doubts as to whether a direct causal relationship between viral infections and A β pathology exists. Analysis of brain tissues from latently HSV-1 infected patients and individuals with HSE did not reveal A β or hyperphosphorylated tau pathology [62]. Moreover, in rare AD patients with HSE, HSV-1 infected cells were frequently found in close proximity to A β plaques but not associated with A β deposition [62]. This pattern closely resembles vicinity but lack of association between HSV-1 infected cells and A β aggregates of 5XFAD in the current work (Figure 3). Finally, in HSE individuals, HSV-1 infected cells did not show an increase in the level of A β [62]. Similarly, in hA β mice with acute HSE, the levels of APP/A β in individual neurons did not change upon HSV-1-infection. In another recent study, a series of experiments examined 5XFAD mice infected with murine roseolovirus (MRV) via two different routes (peripheral/intracranial) at various time points (before/after spontaneous formation of A β plaques); the mice were analyzed at multiple time-points post infection (acute/chronic) [63]. In young 5XFADs, MRV infection did not induce the formation of A β plaques de novo [63]. In older 5XFAD mice with A β pathology, MRV infection did not increase the plaque density nor facilitate the progression of A β pathology [63]. Our previous studies showed that the 5XFAD genotype failed to protect 6-week-old mice challenged IC with three different doses of McKrae or 17syn+ HSV-1 strains that were above or below the LD₅₀ value [38]. No A β aggregates could be found in young 5XFAD that succumbed to acute HSE or in the survivors, 2 or 7.5 weeks postinoculation. In 7- to 10-month-old and 12- to 15-month-old 5XFAD cohorts challenged via IC route with McKrae, a high density of extracellular A β aggregates did not change the time course or outcomes of viral infection when compared with that of WT littermates [38]. Moreover, in aged 5XFADs, A β aggregates were free of HSV-1 too.

Several limitations of the current work have to be discussed. The current study does not address whether A β pathology could be triggered by latent HSV-1 infection with multiple re-activation events. In previous studies, latent HSV-1 infection of BALB/c mice subjected to repetitive cycles of reactivation led to behavioral deficits along with AD-like pathology including phosphorylation of tau, neuroinflammation and A β plaques, as detected by Thioflavin S [14]. In humans, A β pathology and hyperphosphorylated tau were not detected in latently HSV-1-infected neurons of either AD patients or control

individuals [62]. To resolve these controversial results, further studies using animal models are needed, which are hindered due to difficulties in establishing latent HSV-1 infection in mice. The work by Eimer and co-workers claims that in 5XFADs, HSV-1 induces A β aggregates within 72 h postinfection [7]. In the current work, hA β mice that survived HSV-1 challenge were followed for as far out as 42 days postinfection; no A β pathology could be observed in surviving mice or those that succumbed to acute HSE. We do not know, whether A β aggregates could be found, if mice were observed longer than 42 days. If this is were true, it is unlikely that direct seeding by HSV-1 would be responsible for plaque formation, because HSV-1 was completely cleared within 2 weeks postinfection in surviving mice. We also do not know whether the hA β mice are capable of developing A β pathology under any circumstances or whether they are resistant to brain amyloid plaques. Aged 22- to 24-month-old hA β mice did not show any A β aggregation or plaques.

In hA β mice, aberrant splicing of Trem2*R47H reduces its expression level to approximately 50% of its normal level, raising concerns that a deficiency in microglial phagocytic functions make this model resistant to chronic neurodegeneration [47, 58]. Indeed, hA β is a relatively new model that has never been shown to develop chronic neurodegeneration, whether spontaneously or in response to an external insult. The antimicrobial hypothesis proposes that A β peptides manifest antimicrobial activity via directly entrapping pathogens, leaving the role of microglia in A β -pathogen interaction poorly defined. Deficiency in microglial phagocytic activity, if such is intrinsic to the hA β model, should facilitate A β plaque formation, as microglia are known to clear A β peptides, fibrils and plaques [64–67]. Nevertheless, for examining the susceptibility of hA β mice to develop chronic neurodegeneration in response to an infectious agent, they were challenged with prions. In hA β mice, the incubation time to terminal disease was slightly shorter relative to C57Bl.6 J cohorts. Like C57Bl.6 J mice, the hA β model displayed widespread neuroinflammation along with phagocytosis of PrP^{Sc} and neurons. These results argue that the hA β model is susceptible to chronic neurodegeneration, and its microglia can acquire a phagocytic phenotype. Upon eye scarification, the hA β cohort showed very similar survival curves to 5XFADs and their WT littermates. The same brain areas were affected by the virus regardless of the differences in APP or Trem2 variants or expression levels in mice of three genotypes. These results also suggest that host-pathogen interactions were not influenced by genotype.

While the current work cannot rule out the hypothesis on the involvement of HSV-1 in the etiology of late-onset AD, our findings do not support the proposition on the protective role of A β against viral infection of the CNS. Moreover, the current results argue against a direct causative relationship between HSV-1 infection and A β

pathology. Nevertheless, alternative mechanisms that do not depend on direct pathogen-triggered formation of A β plaques should be considered for explaining an increased risk to late onset AD in individuals with viral infections of the CNS [68]. For instance, recurrent reactivation of latent infection or repetitive exposure to viruses can lead to chronic neuroinflammation, which has been recognized as one of the drivers of chronic neurodegeneration [69].

Acute HSV-1 infection is known to elicit a robust innate immune response that involves resident microglia, astrocytes and infiltrating immune cells [70–72]. Resident microglia and astrocytes recognize HSV-1 via pattern-recognition receptors (PRPs) and, in response to HSV-1, express a cocktail of cytokines and chemokines including CCL2, which signal to recruit peripheral myeloid cells into the sites of infection [71]. Extensive infiltration of peripheral myeloid cells during the acute phase of HSV-1 infection seen in the current studies is in agreement with previous results documenting infiltration of macrophages and T lymphocytes during early stages of brain invasion by HSV-1 [70, 73]. Notably, early infiltration by myeloid cells was followed by prolonged activation of resident microglia and retention of T lymphocytes [73]. The contribution of HSV-1-induced microglia activation and the effect of long-term retention of T lymphocyte in the etiology of late onset AD remains to be examined.

Both microglia and infiltrating myeloid cells exhibit phagocytic activities, and because the latter were shown to express microglia-specific markers upon differentiation in brain parenchyma, defining the cell type responsible for phagocytic uptake of infected neurons has been difficult [74]. The current work supports the results of recent studies that Gal3 is a specific marker of infiltrating monocytes [49]. Moreover, our work revealed that a large fraction of infiltrating myeloid cells remained Iba1 negative at least within the first few days of residing in brain parenchyma. Phagocytic uptake of HSV-1 infected neurons was associated with both resident microglia and infiltrating myeloid cells. However, in response to acute infection, the phagocytic activity of resident microglia did not increase significantly, but only showed an upward trend. Surprisingly, a significant population of infiltrating myeloid cells (CD45^{hi}CD11b⁺Ly6C⁺) displayed the neuronal marker NeuN along with the phagocytic marker, CD68. High phagocytic activity of infiltrating myeloid cells was evident from the bead engulfment assay. Considering the 91-fold increase in population of peripheral myeloid cells, our data suggests that phagocytic activity of infiltrating myeloid cells constitutes the primary defense mechanism against HSV-1 during the acute phase.

The current work supports the view that the primary mechanism responsible for clearing viral infections of the CNS involves phagocytic uptake of infected neurons by myeloid cells whether resident or infiltrating [46]. Notably, several recent studies pointed at a dual role for

myeloid cells in the pathogenesis of AD. Not only do microglia phagocytose A β aggregates, but phagocytes can also promote the formation of A β plaques via uptake and condensing A β peptides into dense deposits or mini-plaques in lysosomes and sprinkling A β seeds around the brain [75, 76]. Phagocytic uptake of infected neurons could also explain the association of viral DNA with A β plaques in AD brains [15]. If this is the case, it would be interesting to test whether phagocytic uptake of infected neurons generates A β mini-plaques as a side product of phagocytosis.

AUTHOR CONTRIBUTIONS

Olga V. Bocharova and Ilia V. Baskakov conceived and designed the study. Olga V. Bocharova, Aidan Fisher, Narayan P. Pandit, Kara Molesworth, Olga Mychko, Natallia Makarava, and Rodney Ritzel conducted the experiments. Olga V. Bocharova, Aidan Fisher, Natallia Makarava, Rodney Ritzel, Ilia V. Baskakov analyzed and interpreted the data. Alison J. Scott contributed reagents. Ilia V. Baskakov wrote the manuscript. All authors approved the article.

ACKNOWLEDGMENT

Research reported in this publication was supported by Microbial Pathogenesis in Alzheimer's Diseases grant from IDSA Foundation.

CONFLICT OF INTEREST

The authors declare no conflict of interests.

DATA AVAILABILITY STATEMENT

The data that support the findings of this study are available upon reasonable request.

ORCID

Ilia V. Baskakov  <https://orcid.org/0000-0003-2821-0942>

REFERENCES

1. Glenner GG, Wong CW. Alzheimer's disease: initial report of the purification and characterization of a novel cerebrovascular amyloid protein. *Biochem Biophys Res Commun.* 1984;120:885–90.
2. Goate A, Chartier-Harlin MC, Mullan M, Brown J, Crawford F, Fidani L, et al. Segregation of a missense mutation in the amyloid precursor protein gene with familial Alzheimer's disease. *Nature.* 1991;349:704–6.
3. Hardy JA, Higgins GA. Alzheimer's disease: the amyloid cascade hypothesis. *Science.* 1992;256(5054):184–5.
4. Piacentini R, De Chiara G, Li Puma DD, Ripoli C, Marcocci ME, Garaci E, et al. HSV-1 and Alzheimer's disease: more than a hypothesis. *Front Pharmacol.* 2014;5:97.
5. Itzhaki RF, Wozniak MA, Appelt DM, Balin BJ. Infiltration of the brain by pathogens causes Alzheimer's disease. *Neurobiol Aging.* 2004;25(5):619–27.
6. De Chiara G, Marcocci ME, Sgarbanti R, Civitelli L, Ripoli C, Piacentini R, et al. Infectious agents and neurodegeneration. *Mol Neurobiol.* 2012;46(3):614–38.
7. Eimer WA, Vijaya Kumar DK, Navalpur Shanmugam NK, Rodriguez AS, Mitchell T, Washicosky KJ, et al. Alzheimer's

- disease-associated β -amyloid is rapidly seeded by herpesviridae to protect against brain infection. *Neuron*. 2018;99(1):56–63.e53.
8. Ezzat K, Pernemalm M, Pålsson S, Roberts TC, Järver P, Dondalska A, et al. The viral protein corona directs viral pathogenesis and amyloid aggregation. *Nat Commun*. 2019;10(1):2331.
 9. Kumar DKV, Choi SH, Washicosky KJ, Eimer WA, Tucker S, Ghofrani J, et al. Amyloid- β peptide protects against microbial infection in mouse and worm models of Alzheimer's disease. *Sci Transl Med*. 2016;8(340):340ra372.
 10. Moir RD, Lathe R, Tanzi RE. The antimicrobial protection hypothesis of Alzheimer's disease. *Alzheimers Dement*. 2018;14(12):1602–14.
 11. Letenneur L, Pérès K, Fleury H, Garrigue I, Barberger-Gateau P, Helmer C, et al. Seropositivity to herpes simplex virus antibodies and risk of Alzheimer's disease: a population-based cohort study. *PLoS One*. 2008;3(11):e3637.
 12. Mancuso R, Baglio F, Agostini S, Agostini MC, Laganà MM, Hernis A, et al. Relationship between herpes simplex virus-1-specific antibody titers and cortical brain damage in Alzheimer's disease and amnesic mild cognitive impairment. *Front Aging Neurosci*. 2014;6:285.
 13. Lövheim H, Gilthorpe J, Adolfsson R, Nilsson L-G, Elgh F. Reactivated herpes simplex infection increases the risk of Alzheimer's disease. *Alzheimers Dement*. 2015;11(6):593–9.
 14. De Chiara G, Piacentini R, Fabiani M, Mastrodonato A, Marcocci ME, Limongi D, et al. Recurrent herpes simplex virus-1 infection induces hallmarks of neurodegeneration and cognitive deficits in mice. *PLoS Pathog*. 2019;15(3):e1007617.
 15. Wozniak MA, Mee AP, Itzhaki RF. Herpes simplex virus type 1 DNA is located within Alzheimer's disease amyloid plaques. *J Pathol*. 2009;217(1):131–8.
 16. Wozniak MA, Frost AL, Itzhaki RF. Alzheimer's disease-specific tau phosphorylation is induced by herpes simplex virus type 1. *J Alzheimers Dis*. 2009;16(2):341–50.
 17. Shipley SJ, Parkin ET, Itzhaki RF, Dobson CB. Herpes simplex virus interferes with amyloid precursor protein processing. *BMC Microbiol*. 2005;5(1):48.
 18. De Chiara G, Marcocci ME, Civitelli L, Argnani R, Piacentini R, Ripoli C, et al. APP processing induced by herpes simplex virus type 1 (HSV-1) yields several APP fragments in human and rat neuronal cells. *PLoS One*. 2010;5(11):e13989.
 19. Piacentini R, Civitelli L, Ripoli C, Marcocci ME, De Chiara G, Garaci E, et al. HSV-1 promotes Ca²⁺-mediated APP phosphorylation and A β accumulation in rat cortical neurons. *Neurobiol Aging*. 2011;32(12):2323.e2313–26.
 20. Li Puma DD, Piacentini R, Leone L, Gironi K, Marcocci ME, De Chiara G, et al. Herpes simplex virus type-1 infection alters adult hippocampal neurogenesis via amyloid- β protein accumulation. *Stem Cells*. 2019;37:1467–80.
 21. Piacentini R, Li Puma DD, Ripoli C, Elena Marcocci M, De Chiara G, Garaci E, et al. Herpes simplex virus type-1 infection induces synaptic dysfunction in cultured cortical neurons via GSK-3 activation and intraneuronal amyloid- β protein accumulation. *Sci Rep*. 2015;5:15444.
 22. Santana S, Recuero M, Bullido MJ, Valdivieso F, Aldudo J. Herpes simplex virus type I induces the accumulation of intracellular β -amyloid in autophagic compartments and the inhibition of the non-amyloidogenic pathway in human neuroblastoma cells. *Neurobiol Aging*. 2012;33(2):430.e419–33.
 23. Álvarez G, Aldudo J, Alonso M, Santana S, Valdivieso F. Herpes simplex virus type 1 induces nuclear accumulation of hyperphosphorylated tau in neuronal cells. *J Neurosci Res*. 2012;90(5):1020–9.
 24. Readhead B, Haure-Mirande J-V, Funk CC, Richards MA, Shannon P, Haroutunian V, et al. Multiscale analysis of independent Alzheimer's cohorts finds disruption of molecular, genetic, and clinical networks by human herpesvirus. *Neuron*. 2018;99(1):64–82.e67.
 25. Jeong H-H, Liu Z. Are HHV-6A and HHV-7 really more abundant in Alzheimer's disease? *Neuron*. 2019;104(6):1034–5.
 26. Allnutt MA, Johnson K, Bennett DA, Connor SM, Troncoso JC, Pletnikova O, et al. Human herpesvirus 6 detection in Alzheimer's disease cases and controls across multiple cohorts. *Neuron*. 2020;105(6):1027–35.
 27. Benzinger TLS, Blazey T, Jack CR, Koeppe RA, Su Y, Xiong C, et al. Regional variability of imaging biomarkers in autosomal dominant Alzheimer's disease. *Proc Natl Acad Sci*. 2013;110(47):E4502–9.
 28. Selkoe DJ, Hardy J. The amyloid hypothesis of Alzheimer's disease at 25 years. *EMBO Mol Med*. 2016;8(6):595–608.
 29. Tachibana M, Holm ML, Liu CC, Shinohara M, Aikawa T, Oue H, et al. APOE4-mediated amyloid- β pathology depends on its neuronal receptor LRP1. *J Clin Invest*. 2019;129(3):1272–7.
 30. Liu CC, Zhao N, Fu Y, Wang N, Linares C, Tsai CW, et al. ApoE4 accelerates early seeding of amyloid pathology. *Neuron*. 2017;96(5):1024–1032.e1023.
 31. Makarava N, Chang JC-Y, Molesworth K, Baskakov IV. Post-translational modifications define course of prion strain adaptation and disease phenotype. *J Clin Invest*. 2020;130(8):4382–95.
 32. Makarava N, Mychko O, Chang JC-Y, Molesworth K, Baskakov IV. The degree of astrocyte activation is predictive of the incubation time to prion disease. *Acta Neuropathol Commun*. 2021;9(1):87.
 33. Hirschfeld M, Ma Y, Weis JH, Vogel SN, Weis JJ. Cutting edge: repurification of lipopolysaccharide eliminates signaling through both human and murine toll-like receptor 2. *J Immunol*. 2000;165(2):618–22.
 34. Ritzel RM, Patel AR, Grenier JM, Crapser J, Verma R, Jellison ER, et al. Functional differences between microglia and monocytes after ischemic stroke. *J Neuroinflammation*. 2015;12:106.
 35. Oakley H, Cole SL, Logan S, Maus E, Shao P, Craft J, et al. Intra-neuronal β -amyloid aggregates, neurodegeneration, and neuron loss in transgenic mice with five familial Alzheimer's disease mutations: potential factors in amyloid plaque formation. *J Neurosci*. 2006;26(40):10129–40.
 36. Marcocci ME, Napoletani G, Protto V, Kolesova O, Piacentini R, Li Puma DD, et al. Herpes simplex virus-1 in the brain: the dark side of a sneaky infection. *Trends Microbiol*. 2020;28(10):808–20.
 37. Drayman N, Patel P, Vistain L, Tay S. HSV-1 single-cell analysis reveals the activation of anti-viral and developmental programs in distinct sub-populations. *Elife*. 2019;8:e46339.
 38. Bocharova O, Pandit NP, Molesworth K, Fisher A, Mychko O, Makarava N, et al. Alzheimer's disease-associated β -amyloid does not protect against herpes simplex virus 1 infection in the mouse brain. *J Biol Chem*. 2021;297(1):100845.
 39. Hs K, Kim S, Shin SJ, Park YH, Nam Y, Cw K, et al. Gram-negative bacteria and their lipopolysaccharides in Alzheimer's disease: pathologic roles and therapeutic implications. *Transl Neurodegener*. 2021;10(1):49.
 40. Qin L, Wu X, Block ML, Liu Y, Breese GR, Hong JS, et al. Systemic LPS causes chronic neuroinflammation and progressive neurodegeneration. *Glia*. 2007;55(5):453–62.
 41. Wang LM, Wu Q, Kirk RA, Horn KP, Ebada Salem AH, Hoffman JM, et al. Lipopolysaccharide endotoxemia induces amyloid- β and p-tau formation in the rat brain. *Am J Nucl Med Mol Imaging*. 2018;8(2):86–99.
 42. Lee JW, Lee YK, Yuk DY, Choi DY, Ban SB, Oh KW, et al. Neuro-inflammation induced by lipopolysaccharide causes cognitive impairment through enhancement of beta-amyloid generation. *J Neuroinflammation*. 2008;5(1):37.
 43. McCormick W, Mermel LA. The basic reproductive number and particle-to-plaque ratio: comparison of these two parameters of viral infectivity. *Virology*. 2021;18(1):92.
 44. Wang H, Davido DJ, Morrison LA. HSV-1 strain McKrae is more neuroinvasive than HSV-1 KOS after corneal or vaginal inoculation in mice. *Virus Res*. 2013;173(2):436–40.

45. Chowdhury S, Naderi M, Chouljenko VN, Walker JD, Kousoulas KG. Amino acid differences in glycoproteins B (gB), C (gC), H (gH) and L (gL) are associated with enhanced herpes simplex virus type-1 (McKrae) entry via the paired immunoglobulin-like type-2 receptor α . *Virology*. 2012;9:112.
46. Fekete R, Cserép C, Lénárt N, Tóth K, Orsolits B, Martincz B, et al. Microglia control the spread of neurotropic virus infection via P2Y12 signalling and recruit monocytes through P2Y12-independent mechanisms. *Acta Neuropathol*. 2018;136(3):461–82.
47. Xiang X, Piers TM, Wefers B, Zhu K, Mallach A, Brunner B, et al. The Trem2 R47H Alzheimer's risk variant impairs splicing and reduces Trem2 mRNA and protein in mice but not in humans. *Mol Neurodegener*. 2018;13(1):49.
48. Sinha A, Kushwaha R, Molesworth K, Mychko O, Makarava N, Baskakov IV. Phagocytic activities of reactive microglia and astrocytes associated with prion diseases are dysregulated in opposite directions. *Cell*. 2021;10(7):1728.
49. Hohsfield LA, Tsourmas KI, Ghorbanian Y, Syage AR, Jin Kim S, Cheng Y, et al. MAC2 is a long-lasting marker of peripheral cell infiltrates into the mouse CNS after bone marrow transplantation and coronavirus infection. *Glia*. 2022;70:875–91.
50. Harris SA, Harris EA. Molecular mechanisms for herpes simplex virus type 1 pathogenesis in Alzheimer's disease. *Front Aging Neurosci*. 2018;10:48.
51. Itzhaki RF. Corroboration of a major role for herpes simplex virus type 1 in Alzheimer's disease. *Front Aging Neurosci*. 2018;10:324.
52. Burgos JS, Ramirez C, Sastre I, Valdivieso F. Effect of apolipoprotein E on the cerebral load of latent herpes simplex virus type 1 DNA. *J Virol*. 2006;80(11):5383–7.
53. Burgos JS, Ramirez C, Sastre I, Bullido MJ, Valdivieso F. ApoE4 is more efficient than E3 in brain access by herpes simplex virus type 1. *Neuroreport*. 2003;14:1825–7.
54. Bhattacharjee PS, Neumann DM, Foster TP, Bouhanik S, Clement C, Vinay D, et al. Effect of human apolipoprotein E genotype on the pathogenesis of experimental ocular HSV-1. *Exp Eye Res*. 2008;87(2):122–30.
55. Hill JM, Bhattacharjee PS, Neumann DM. Apolipoprotein E alleles can contribute to the pathogenesis of numerous clinical conditions including HSV-1 corneal disease. *Exp Eye Res*. 2007;84(5):801–11.
56. Itzhaki RF, Lin W-R, Shang D, Wilcock GK, Faragher B, Jamieson GA. Herpes simplex virus type 1 in brain and risk of Alzheimer's disease. *The Lancet*. 1997;349(9047):241–4.
57. Marques AR, Straus SE, Fahle G, Weir S, Csako G, Fischer SH. Lack of association between HSV-1 DNA in the brain, Alzheimer's disease and apolipoprotein E4. *J Neurovirol*. 2001;7(1):82–3.
58. Kotredes KP, Oblak A, Pandey RS, Lin PB-C, Garceau D, Williams H, et al. Uncovering disease mechanisms in a novel mouse model expressing humanized APOE ϵ 4 and Trem2*R47H. *Front Aging Neurosci*. 2021;13:735524.
59. Kollias CM, Huneke RB, Wigdahl B, Jennings SR. Animal models of herpes simplex virus immunity and pathogenesis. *J Neurovirol*. 2015;21(1):8–23.
60. Webre JM, Hill JM, Nolan NM, Clement C, McFerrin HE, Bhattacharjee PS, et al. Rabbit and mouse models of HSV-1 latency, reactivation, and recurrent eye diseases. *J Biomed Biotechnol*. 2012;2012:612316.
61. Sawtell NM, Poon DK, Tansky CS, Thompson RL. The latent herpes simplex virus type 1 genome copy number in individual neurons is virus strain specific and correlates with reactivation. *J Virol*. 1998;72(7):5343–50.
62. Tran DN, Bakx A, van Dis V, Aronica E, Verdijk RM, Ouwendijk WJD. No evidence of aberrant amyloid β and phosphorylated tau expression in herpes simplex virus-infected neurons of the trigeminal ganglia and brain. *Brain Pathol*. 2021;32(4):e13044.
63. Bigley TM, Xiong M, Ali M, Chen Y, Wang C, Serrano JR, et al. Murine roseolovirus does not accelerate amyloid- β pathology and human roseoloviruses are not over-represented in Alzheimer disease brains. *Mol Neurodegener*. 2022;17(1):10.
64. Ries M, Sastre M. Mechanisms of A β clearance and degradation by glial cells. *Front Aging Neurosci*. 2016;8:160.
65. Koenigsnecht J, Landreth G. Microglial phagocytosis of fibrillar beta-amyloid through a beta1 integrin-dependent mechanism. *J Neurosci*. 2004;24(44):9838–46.
66. Mandrekar S, Jiang Q, Lee CY, Koenigsnecht-Talboo J, Holtzman DM, Landreth GE. Microglia mediate the clearance of soluble A β through fluid phase macropinocytosis. *J Neurosci*. 2009;29(13):4252–62.
67. Rivera-Escalera F, Pinney JJ, Owlett L, Ahmed H, Thakar J, Olschowka JA, et al. IL-1 β -driven amyloid plaque clearance is associated with an expansion of transcriptionally reprogrammed microglia. *J Neuroinflammation*. 2019;16(1):261.
68. Tzeng N-S, Chung C-H, Lin F-H, Chiang C-P, Yeh C-B, Huang S-Y, et al. Anti-herpetic medications and reduced risk of dementia in patients with herpes simplex virus infections: a nationwide, population-based cohort study in Taiwan. *Neurotherapeutics*. 2018;15(2):417–29.
69. Frank-Cannon TC, Alto LT, McAlpine FE, Tansey MG. Does neuroinflammation fan the flame in neurodegenerative diseases? *Mol Neurodegener*. 2009;4(1):47.
70. Menasria R, Canivet C, Piret J, Boivin G. Infiltration pattern of blood monocytes into the central nervous system during experimental herpes simplex virus encephalitis. *PLoS One*. 2015;10(12):e0145773.
71. Brun P, Scarpa M, Marchiori C, Conti J, Kotsafti A, Porzionato A, et al. Herpes simplex virus type 1 engages toll like receptor 2 to recruit macrophages during infection of enteric neurons. *Front Microbiol*. 2018;9:2148.
72. Paludan SR, Bowie AG, Horan KA, Fitzgerald KA. Recognition of herpesviruses by the innate immune system. *Nat Rev Immunol*. 2011;11(2):143–54.
73. Marques R, Antunes I, Eksmond U, Stoye J, Hasenkrug K, Kassiotis G. B lymphocyte activation by coinfection prevents immune control of friend virus infection. *J Immunol*. 2008;181(5):3432–40.
74. Andoh M, Koyama R. Comparative review of microglia and monocytes in CNS phagocytosis. *Cell*. 2021;10(10):2555.
75. Huang Y, Happonen KE, Burrola PG, O'Connor C, Hah N, Huang L, et al. Microglia use TAM receptors to detect and engulf amyloid β plaques. *Nat Immunol*. 2021;22:586–94.
76. d'Errico P, Ziegler-Waldkirch S, Aires V, Hoffmann P, Mezö C, Erny D, et al. Microglia contribute to the propagation of A β into unaffected brain tissue. *Nat Neurosci*. 2022;25(1):20–5.

SUPPORTING INFORMATION

Additional supporting information can be found online in the Supporting Information section at the end of this article.

How to cite this article: Bocharova OV, Fisher A, Pandit NP, Molesworth K, Mychko O, Scott AJ, et al. A β plaques do not protect against HSV-1 infection in a mouse model of familial Alzheimer's disease, and HSV-1 does not induce A β pathology in a model of late onset Alzheimer's disease. *Brain Pathology*. 2023;33(1):e13116. <https://doi.org/10.1111/bpa.13116>